大阪大學 Jan. 30, 2011 @Ascona

How to find and synthesize new multiferroics showing strong magnetoelectric coupling

Tsuyoshi Kimura

Division of Materials Physics,
Graduate School of Engineering Science
Osaka University

---

from web site of 2001 American Physical Society March meeting @ Seattle

Session C21. DMP: Multiferroics II.
Monday morning, 11:00, 12 March 2001, Room 604, Washington State Convention Center

C21.001 Materials being simultaneously ferroelectric, ferromagnetic, ferrotoroidic and ferroelastic
Hans Schmid (University of Geneva, CH-1211 Geneva 4, Switzerland)

C21.002 Magnetism and ferroelectricity; why do they so seldom coexist?
Daniel Khomskii (Groningen University, The Netherlands)

C21.003 Biferroic (ferroelectric-ferroelastic) Characteristics of Oriented Piezoelectric Crystals
Dwight Viehland (Dept. of the Navy)

C21.004 Study of stress induced polarization switching in ferroelectrics using 2-D simulation
Rajeev Ahluwalia, Wenwu Cao (Pennsylvania State University)

C21.005 Piezoelectric characterization of Ferrite/Ferroelectric magnetoelectric composite system.
Srinivas Kuchipudi, Prasad Goduru, S.V Suryanarayana (Osmania University, Hyderabad-7, INDIA)

C21.006 Prediction of coupling magnetoelectric effect in ferromagnetic rare-earth-iron alloys
Ce-Wen Nan (Tsinghua University, Beijing 100084, China)

C21.007 Why are there so few magnetic ferroelectrics?
Nicola Hill (University of California at Santa Barbara)

C21.008 A Thermodynamic Theory for a Multiferroic
Avadh Saxena (Los Alamos National Laboratory), Pradeep Kumar (University of Florida)

Outline of this lecture

- Symmetry in crystals
- Magnetic symmetry
- Conventional magnetoelectric effect
- Single crystal growth
- Spin-spiral-driven multiferroics
  - Orthorhombic perovskite manganites $RMnO_3$
  - Cuprates and ferrites working at room temperature
- Observation of spin-spiral domain structure
- ME effect in magnetically-disordered system

Symmetry operations

There are 4 kinds of geometric symmetry operations.

Translation

$(x,y,z) \rightarrow (x+x_1, y+y_1, z+z_1)$

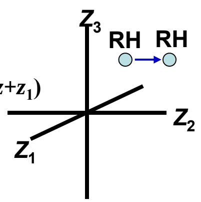

Mirror *m*

$(x,y,z) \rightarrow (x,-y,z)$

Direction cosine matrix

$m \perp Z_2 \quad (a) = \begin{pmatrix} 1 & 0 & 0 \\ 0 & -1 & 0 \\ 0 & 0 & 1 \end{pmatrix}$

$|a| = -1$

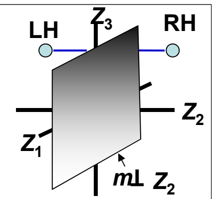

A mirror plane is a 2D symmetry element that reverses the sign of one coordinate.

Rotation 2, 3, 4, 6

$(x,y,z) \rightarrow (-x,-y,z)$

Direction cosine matrix

$2 \,//\, Z_3 \quad (a) = \begin{pmatrix} -1 & 0 & 0 \\ 0 & -1 & 0 \\ 0 & 0 & 1 \end{pmatrix}$

$|a| = +1$

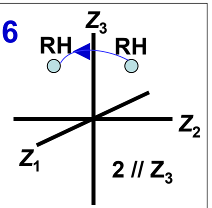

Rotation axes are 1D symmetry elements that change two coordinates.

Inversion $\bar{1}$

$(x,y,z) \rightarrow (-x,-y,-z)$

Direction cosine matrix

$\bar{1} \quad \begin{pmatrix} -1 & 0 & 0 \\ 0 & -1 & 0 \\ 0 & 0 & -1 \end{pmatrix}$

$|a| = -1$

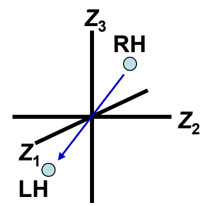

Inversion center is a zero-D point that change all three coordinates.

Mirror & Inversion transformations are accompanied by a handedness change, while rotation & translation are not.

Stereographic projections

To visualize point groups, we make use of stereographic projections.

→ Easy way of representing 3D objects in 2D

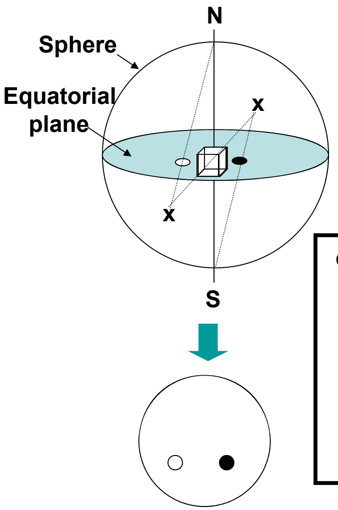

1. An object located at the center of sphere
2. Any point of interest is then projected to the surface.
3. If the point ends in the northern hemisphere, then connecting it to the South Pole.
4. Where this line intersects the equatorial plane is the point on the stereographic projection.
5. Closed (open) circles identify points originating from the northern (southern) hemispheres.

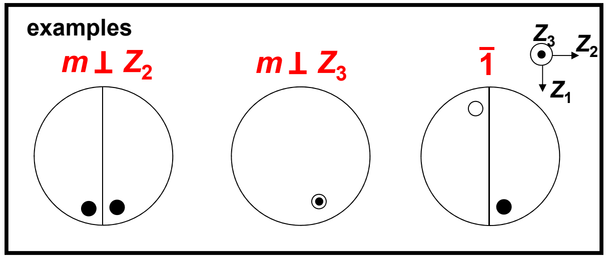

32 point groups illustrated by stereograms

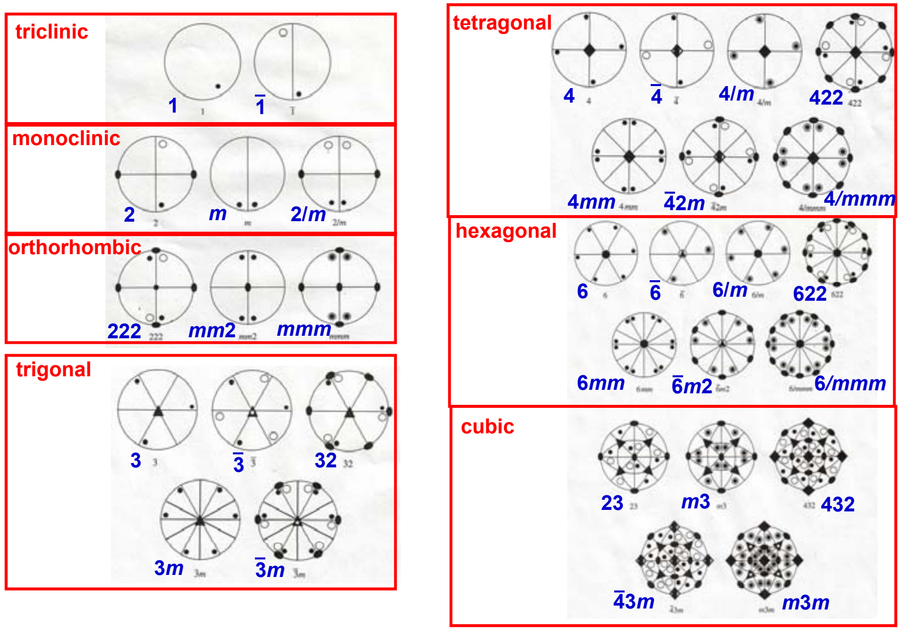

Transformation operators for symmetry elements

The 14 symmetry elements generate the 32 point group

Identity operator — 1 $\begin{pmatrix} 1 & 0 & 0 \\ 0 & 1 & 0 \\ 0 & 0 & 1 \end{pmatrix}$

Inversion center — $\bar{1}$ $\begin{pmatrix} -1 & 0 & 0 \\ 0 & -1 & 0 \\ 0 & 0 & -1 \end{pmatrix}$

Twofold rotation (2) parallel to Z_1 — $2 // Z_1$ $\begin{pmatrix} 1 & 0 & 0 \\ 0 & -1 & 0 \\ 0 & 0 & -1 \end{pmatrix}$

Twofold rotation (2) parallel to Z_2 — $2 // Z_2$ $\begin{pmatrix} -1 & 0 & 0 \\ 0 & 1 & 0 \\ 0 & 0 & -1 \end{pmatrix}$

Mirror (*m*) perpendicular to Z_1 — $m \perp Z_1$ $\begin{pmatrix} -1 & 0 & 0 \\ 0 & 1 & 0 \\ 0 & 0 & 1 \end{pmatrix}$

Mirror (*m*) perpendicular to Z_2 — $m \perp Z_2$ $\begin{pmatrix} 1 & 0 & 0 \\ 0 & -1 & 0 \\ 0 & 0 & 1 \end{pmatrix}$

Mirror (*m*) perpendicular to Z_3 — $m \perp Z_3$ $\begin{pmatrix} 1 & 0 & 0 \\ 0 & 1 & 0 \\ 0 & 0 & -1 \end{pmatrix}$

Threefold rotation (3) parallel to Z_3 — $3 // Z_3$ $\begin{pmatrix} -1/2 & \sqrt{3}/2 & 0 \\ -\sqrt{3}/2 & -1/2 & 0 \\ 0 & 0 & 1 \end{pmatrix}$

Threefold rotation (3) parallel to [111] — $3 // [111]$ $\begin{pmatrix} 0 & 1 & 0 \\ 0 & 0 & 1 \\ 1 & 0 & 0 \end{pmatrix}$

Threefold inversion axis ($\bar{3}$) parallel to Z_3 — $\bar{3} // Z_3$ $\begin{pmatrix} 1/2 & -\sqrt{3}/2 & 0 \\ \sqrt{3}/2 & 1/2 & 0 \\ 0 & 0 & -1 \end{pmatrix}$

Threefold inversion axis ($\bar{3}$) parallel to [111] in cubic crystals — $\bar{3} // [111]$ $\begin{pmatrix} 0 & -1 & 0 \\ 0 & 0 & -1 \\ -1 & 0 & 0 \end{pmatrix}$

Fourfold rotation (4) parallel to Z_3 — $4 // Z_3$ $\begin{pmatrix} 0 & 1 & 0 \\ -1 & 0 & 0 \\ 0 & 0 & 1 \end{pmatrix}$

Fourfold inversion ($\bar{4}$) parallel to Z_3 — $\bar{4} // Z_3$ $\begin{pmatrix} 0 & -1 & 0 \\ 1 & 0 & 0 \\ 0 & 0 & -1 \end{pmatrix}$

Sixfold rotation (6) parallel to Z_3 — $6 // Z_3$ $\begin{pmatrix} 1/2 & \sqrt{3}/2 & 0 \\ -\sqrt{3}/2 & 1/2 & 0 \\ 0 & 0 & 1 \end{pmatrix}$

Sixfold inversion ($\bar{6}$) parallel to Z_3 — $6 // Z_3$ $\begin{pmatrix} -1/2 & -\sqrt{3}/2 & 0 \\ \sqrt{3}/2 & -1/2 & 0 \\ 0 & 0 & -1 \end{pmatrix}$

Minimum symmetry elements for the 32 point groups

Point group	Symmetry elements
1	1
$\bar{1}$	$\bar{1}$
2	$2 \parallel Z_2$
m	$m \perp Z_2$
$2/m$	$2 \parallel Z_2, m \perp Z_2$
222	$2 \parallel Z_1, 2 \parallel Z_2$
$mm2$	$m \perp Z_1, m \perp Z_2$
mmm	$m \perp Z_1, m \perp Z_2, m \perp Z_3$
3	$3 \parallel Z_3$
$\bar{3}$	$\bar{3} \parallel Z_3$
32	$3 \parallel Z_3, 2 \parallel Z_1$
$3m$	$3 \parallel Z_3, m \perp Z_1$
$\bar{3}m$	$\bar{3} \parallel Z_3, m \perp Z_1$
4	$4 \parallel Z_3$
$\bar{4}$	$\bar{4} \parallel Z_3$
$4/m$	$4 \parallel Z_3, m \perp Z_3$
422	$4 \parallel Z_3, 2 \parallel Z_1$
$4mm$	$4 \parallel Z_3, m \perp Z_1$
$\bar{4}2m$	$\bar{4} \parallel Z_3, 2 \parallel Z_1$
$4/mmm$	$4 \parallel Z_3, m \perp Z_3, m \perp Z_1$
6	$6 \parallel Z_3$
$\bar{6}$	$\bar{6} \parallel Z_3$
$6/m$	$6 \parallel Z_3, m \perp Z_3$
622	$6 \parallel Z_3, 2 \parallel Z_1$
$6mm$	$6 \parallel Z_3, m \perp Z_1$
$\bar{6}m2$	$\bar{6} \parallel Z_3, m \perp Z_1$
$6/mmm$	$6 \parallel Z_3, m \perp Z_3, m \perp Z_1$
23	$2 \parallel Z_1, 3 \parallel [111]$
$m3$	$m \perp Z_1, 3 \parallel [111]$
432	$4 \parallel Z_3, 3 \parallel [111]$
$\bar{4}3m$	$\bar{4} \parallel Z_3, 3 \parallel [111]$
$m3m$	$m \perp Z_1, 3 \parallel [111], m \perp [110]$

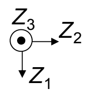

Tensors and physical properties

We introduce the tensor description of physical properties relating symmetry to physical properties.

Tensors are defined by the way in which they transform from one coordinate system to another.

Measured quantities such as STRESS & STRAIN can be represented by tensors.

elastic compliance

Tensors are useful in describing anisotropy of physical properties.

Polar tensors & Axial tensors

→ Their transformation laws are slightly different.

Polar tensors

For a polar tensor, the general transformation law for a tensor of rank N is

$$T'_{ijk\ldots} = a_{il}a_{jm}a_{kn}\ldots T_{lmn\ldots},$$

$T'_{ijk\ldots}$; tensor component in new axial system,
$a_{il}a_{jm}a_{kn}\ldots$; direction cosines,
$T_{lmn\ldots}$, tensor component in old system

$T' = T$
$T_i' = a_{ij}T_j$
$T_{ij}' = a_{ik}a_{jl}T_{kl}$
$T_{ijk}' = a_{il}a_{jm}a_{kn}T_{lmn}$

Each tensor component has N subscripts and there are N direction cosines involved in the product $a_{il}a_{jm}a_{kn}\ldots$.

Meaning of the tensor rank *N*

→ Number of directions involved in measuring the properties

Example; (Thermal conductivity k relates heat flow h to T-gradient dT/dZ)

$h_i = -k_{ij}\,(dT/dZ_j)$ (2 directions in measuring k)

⇩

belongs to materials

h_i and dT/dZ_j are first rank polar tensor quantities, while the thermal conductivity k is a second rank tensor property.

k depends on the symmetry of the material, whereas the heat flow and temperature gradient do not.

Tensor rank of other physical properties

Pyroelectricity p ; a relationship between thermal & electric variables

⇩

A change in temperature ΔT creates a change in electric polarization P. (+ / -)

Polarization → vector (= first rank tensor)

Temperature → scalar (= zero rank tensor)

⇩

$P_i = p_i\Delta T$ (pyroelectric coefficient p_i; first rank tensor property)

Rank	Polar tensor property	
Zero	Specific heat	$C = (\Delta Q/\Delta T)$
First	Pyroelectricity	$P_i = p_i\Delta T$
Second	Thermal expansion	$x_{ij} = \alpha_{ij}\Delta T$
Third	Piezoelectricity	$P_j = d_{jkl}x_{kl}$

The symmetry of any physical property of a crystal must include the symmetry elements of the point group of the crystal.

⇩

The measurements made in symmetry-related directions will give the same property coefficient.

Pyroelectricity

The name is derived from the Greek *pyr*, fire, and electricity.

Pyroelectricity p is a first rank tensor property relating a change electric polarization P to a change in temperature δT. The defining relation can also be written in terms of the electric displacement D since no field is applied.

$$P_i = D_i = p_i\delta T\ [\mathrm{C/m^2}]$$

$$p_i = a_{ij}p_j$$

Symmetry limitations for pyroelectricity (rank 1)

Pyroelectricity disappears in all centrosymmetric materials.

For a first rank tensor there are 3 nonzero coefficients, p_1, p_2, & p_3.

Tensor coefficients are often written in matrix form:

$$\underset{3\times 1}{(p')} = \underset{3\times 3}{(a)}\ \underset{3\times 1}{(p)}$$

$(p') = (p)$ If the direction cosine matrix (a) is a symmetry element of material.

For the inversion symmetry operation we have

$$(p') = \begin{pmatrix} p_1' \\ p_2' \\ p_3' \end{pmatrix} = \begin{pmatrix} -1 & 0 & 0 \\ 0 & -1 & 0 \\ 0 & 0 & -1 \end{pmatrix} \begin{pmatrix} p_1 \\ p_2 \\ p_3 \end{pmatrix} = \begin{pmatrix} -p_1 \\ -p_2 \\ -p_3 \end{pmatrix} = -(p)$$

$$\begin{pmatrix} -p_1 \\ -p_2 \\ -p_3 \end{pmatrix} = \begin{pmatrix} p_1 \\ p_2 \\ p_3 \end{pmatrix}$$

which is only satisfied if all 3 pyroelectric coefficients are zero: $p_1 = p_2 = p_3 = 0$

Pyroelectricity disappears in all point groups containing inversion symmetry.

Example

Is $LiNbO_3$ (point group 3*m*) pyroelectric or not?

If yes, which pyroelectric coefficient p_i can be finite?

Symmetry elements for 3m

$$3 \parallel Z_3 \begin{pmatrix} -1/2 & \sqrt{3}/2 & 0 \\ -\sqrt{3}/2 & -1/2 & 0 \\ 0 & 0 & 1 \end{pmatrix} \qquad m \perp Z_1 \begin{pmatrix} -1 & 0 & 0 \\ 0 & 1 & 0 \\ 0 & 0 & 1 \end{pmatrix}$$

$(p') = (a)\ (p)$

$p_1' = -1/2p_1 + \sqrt{3}/2p_2$

$p_2' = -\sqrt{3}/2p_1 - 1/2p_2$

$p_3' = p_3$

$p_1' = -p_1 \longrightarrow p_1 = 0$

$p_2' = p_2$

$p_3' = p_3$

$p_2' = -1/2p_2$

$\downarrow$

$p_2 = 0$

p_3 can be finite.

by Neumann's Principle,
If the transformation matrix is for symmetry operation,
$(p') = (p)$.

3*m* is pyroelectric with $\begin{pmatrix} 0 \\ 0 \\ p_3 \end{pmatrix}$

Polar axes

Pyroelectric matrices for 10 pyroelectric point groups

The direction of the polar axis is fixed by symmetry.

Point group	
1	$\begin{pmatrix} p_1 \\ p_2 \\ p_3 \end{pmatrix}$
2	$\begin{pmatrix} 0 \\ p_2 \\ 0 \end{pmatrix}$
m	$\begin{pmatrix} p_1 \\ 0 \\ p_3 \end{pmatrix}$
*mm*2, 3, 3*m*, 4, 4*mm*, 6, 6*mm*	$\begin{pmatrix} 0 \\ 0 \\ p_3 \end{pmatrix}$

It is easy to visualize the polar axis directions by examining stereographic projections.

point group: *m* point group: 2 point group: 2/*m*

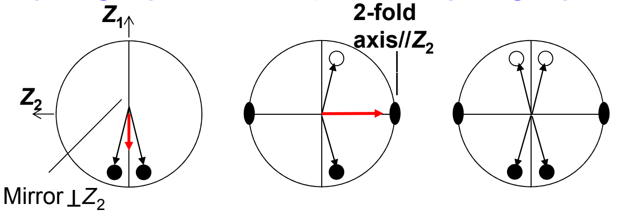

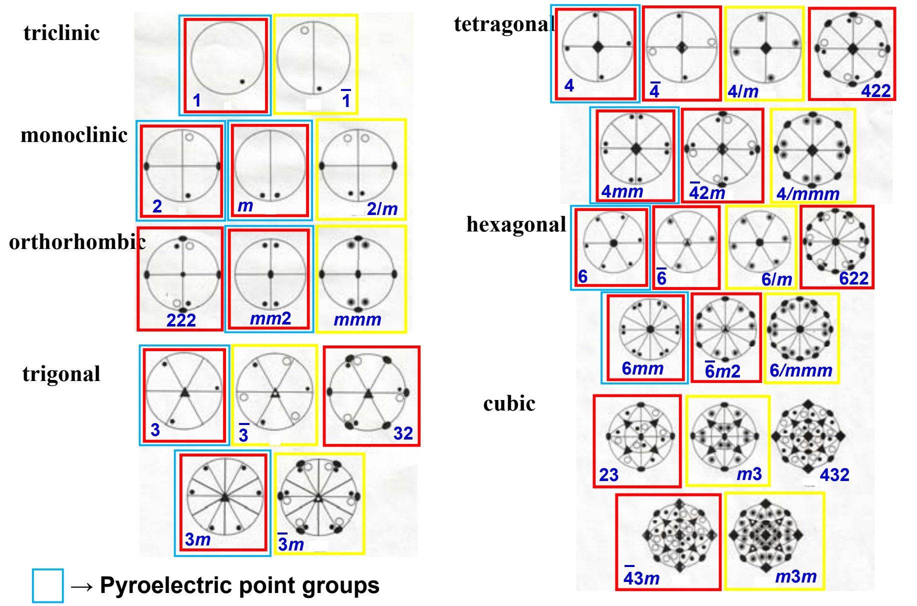

→ **Pyroelectric point groups**

→ **Piezoelectric point groups**

→ **Centrosymmetric point groups**

Axial tensor

Several properties change sign
when the axial system changes from right-handed to left-handed.
(e.g. pyromagnetism, Hall effect …)

Axial tensors ⟶ depends on handedness

Axial tensors transform in the following manner,

$$T'_{ijk\cdots} = |a| a_{il} a_{jm} a_{kn} \cdots T_{lmn\cdots},$$

↑ **Determinant of the direction cosines matrix**

> **$|a|$ = +1 or -1 depending on whether or not the handedness of the axial system changes during transformation**
>
> **For mirror or inversion symmetry operations, $|a|$ =-1 i.e. the sign of the tensor coefficient changes.**

Magnetoelectricity ⟶ ***a second rank axial tensor properties***

A most familiar examples of tensors : vectors (the 1st rank tensors)

	Polar vectors	Axial vectors
characteristics	Displacement (directed segment of length), that is, arrow	Vector product of two polar tensors (the directional properties of element of area, rather than arrow)
examples	electric polarization P electric field E	magnetic moment M magnetic field H
The direction which arrow points (i.e. sign) under handedness change	change	Not change
Effect of inversion operation	Vector which breaks inversion symmetry	Vector which preserves inversion symmetry

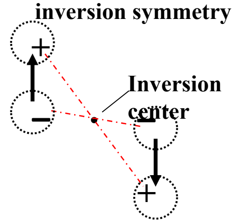

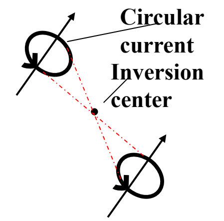

Outline of this lecture

- Symmetry in crystals
- Magnetic symmetry
- Conventional magnetoelectric effect
- Single crystal growth
- Spin-spiral-driven multiferroics
  - Orthorhombic perovskite manganites $RMnO_3$
  - Cuprates and ferrites working at room temperature
- Observation of spin-spiral domain structure
- ME effect in magnetically-disordered system

Symmetries & tensors related to magnetic phenomena

Representative magnetic structures in magnetically ordered materials

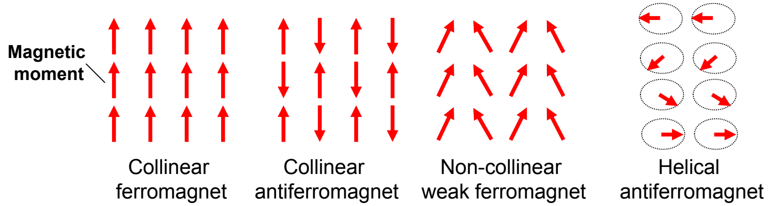

Geometric representations are helpful
in determining the effect of symmetry on physical properties.

Magnetic moments are often visualized as arrows, but this is somewhat misleading.

⇩

Magnetization arises from moving electric charge
so that a current loop is more meaningful symbol.

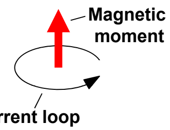

Transformations of a current loop (magnetic moment) under 4 symmetry operations

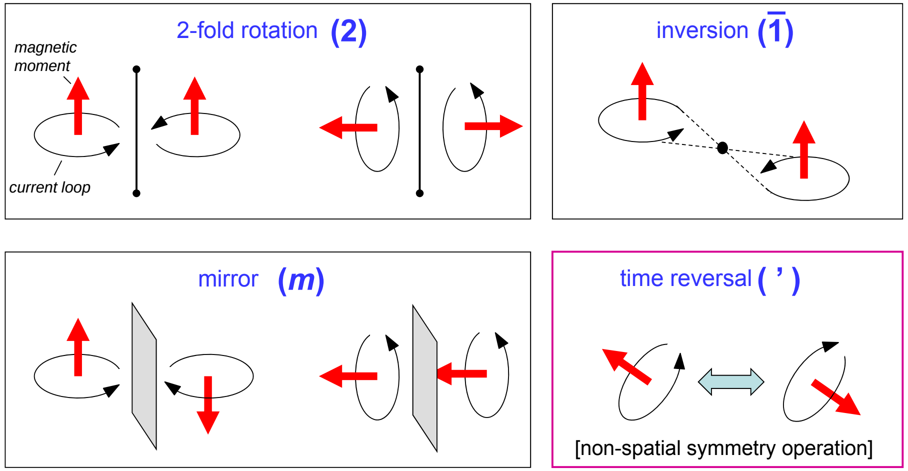

In addition to rotation, mirror inversion operations, time reversal operation can be a symmetry operation in magnetically ordered materials.

Simple examples of magnetic point groups

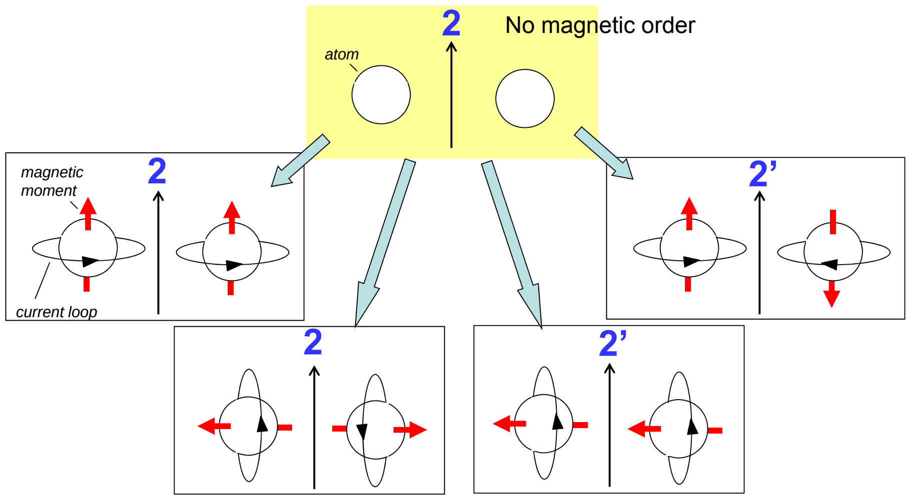

Introduction of the time reversal operator increases the number of classes by adding 90 additional magnetic point groups.

Discussing magnetic symmetry

When discussing magnetic symmetry, it is necessary to distinguish the crystallographic point groups from the magnetic point groups.

2/*m*1' : crystallographic group
(containing both the regular & time-reversed symmetry elements)

4 magnetic point groups associated with crystallographic group 2/*m*1'

- **2/*m* : containing 2, *m*, & $\bar{1}$, but not 2', *m*', and $\bar{1}$'**
- **2/*m*' : containing 2, *m*', & $\bar{1}$'**
- **2'/*m* : containing 2', *m*, & $\bar{1}$'**
- **2'/*m*' : containing 2', *m*', & $\bar{1}$**

Stereograms of the 4 magnetic point groups

Square & circular symbols represent points related by time reversal.

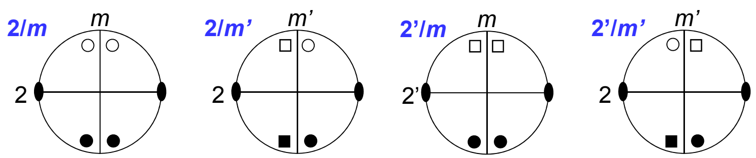

List of magnetic point groups

	Number of nonzero magnetoelectric coefficient	Generating elements
Triclinic		
1	9(9)	1
$\bar{1}$	0	$\bar{1}$
$\bar{1}'$	9(9)	$\bar{1}'$
Monoclinic		
2	5(5)	$2 \parallel Z_2$
$2'$	4(4)	$2' \parallel Z_2$
m	4(4)	$m \perp Z_2$
m'	5(5)	$m' \perp Z_2$
$2/m$	0	$2 \parallel Z_2, m \perp Z_2$
$2'/m'$	0	$2' \parallel Z_2, m' \perp Z_2$
$2/m'$	5(5)	$2 \parallel Z_2, m' \perp Z_2$
$2'/m$	4(4)	$2' \parallel Z_2, m \perp Z_2$
Orthorhombic		
222	3(3)	$2 \parallel Z_2, 2 \parallel Z_3$
$2'2'2$	2(2)	$2' \parallel Z_2, 2 \parallel Z_3$
$mm2$	2(2)	$m \perp Z_2, 2 \parallel Z_3$
$m'm'2$	3(3)	$m' \perp Z_2, 2 \parallel Z_3$
$m'm2'$	2(2)	$m \perp Z_2, 2' \parallel Z_3$
mmm	0	$m \perp Z_1, m \perp Z_2, m \perp Z_3$
$m'm'm$	0	$m' \perp Z_1, m' \perp Z_2, m \perp Z_3$
$m'm'm'$	3(3)	$m' \perp Z_1, m' \perp Z_2, m' \perp Z_3$
$m'mm$	2(2)	$m' \perp Z_1, m \perp Z_2, m \perp Z_3$
Trigonal		
3	5(3)	$3 \parallel Z_3$
$\bar{3}$	0	$\bar{3} \parallel Z_3$
$\bar{3}'$	5(3)	$\bar{3}' \parallel Z_3$
32	3(2)	$2 \parallel Z_1, 3 \parallel Z_3$
$32'$	2(1)	$2' \parallel Z_1, 3 \parallel Z_3$
$3m$	2(1)	$m \perp Z_1, 3 \parallel Z_3$
$3m'$	3(2)	$m' \perp Z_1, 3 \parallel Z_3$
$\bar{3}m$	2(1)	$m \perp Z_1, \bar{3} \parallel Z_3$
$\bar{3}m'$	0	$m' \perp Z_1, \bar{3} \parallel Z_3$
$\bar{3}'m'$	3(2)	$m' \perp Z_1, \bar{3}' \parallel Z_3$
$\bar{3}'m$	0	$m \perp Z_1, \bar{3}' \parallel Z_3$
Tetragonal		
4	5(3)	$4 \parallel Z_3$
$4'$	4(2)	$4' \parallel Z_3$
$\bar{4}$	4(2)	$\bar{4} \parallel Z_3$
$\bar{4}'$	5(3)	$\bar{4}' \parallel Z_3$
$4/m$	0	$m \perp Z_3, 4 \parallel Z_3$
$4'/m$	0	$m \perp Z_3, 4' \parallel Z_3$
$4/m'$	5(3)	$m' \perp Z_3, 4 \parallel Z_3$
$4'/m'$	4(2)	$m' \perp Z_3, 4' \parallel Z_3$
422	3(2)	$2 \parallel Z_1, 4 \parallel Z_3$
$4'22$	2(1)	$2 \parallel Z_1, 4' \parallel Z_3$
$42'2'$	2(1)	$2' \parallel Z_1, 4 \parallel Z_3$
$4mm$	2(1)	$m \perp Z_1, 4 \parallel Z_3$
$4'mm'$	2(1)	$m \perp Z_1, 4' \parallel Z_3$
$4m'm'$	3(2)	$m' \perp Z_1, 4 \parallel Z_3$
$\bar{4}2m$	2(1)	$2 \parallel Z_1, \bar{4} \parallel Z_3$
$\bar{4}'2m'$	3(2)	$2 \parallel Z_1, \bar{4}' \parallel Z_3$
$\bar{4}'2'm$	2(1)	$2' \parallel Z_1, \bar{4}' \parallel Z_3$
$\bar{4}2'm'$	2(1)	$2' \parallel Z_1, \bar{4} \parallel Z_3$
$4/mmm$	0	$m \perp Z_1, m \perp Z_3, 4 \parallel Z_3$
$4'/mmm'$	0	$m \perp Z_1, m \perp Z_3, 4' \parallel Z_3$
$4/mm'm'$	0	$m' \perp Z_1, m \perp Z_3, 4 \parallel Z_3$
$4/m'm'm'$	3(2)	$m' \perp Z_1, m' \perp Z_3, 4 \parallel Z_3$
$4/m'mm$	2(1)	$m \perp Z_1, m' \perp Z_3, 4 \parallel Z_3$
$4'/m'mm'$	2(1)	$m \perp Z_1, m' \perp Z_3, 4' \parallel Z_3$
Hexagonal		
6	5(3)	$6 \parallel Z_3$
$6'$	0	$6' \parallel Z_3$
$\bar{6}$	0	$\bar{6} \parallel Z_3$
$\bar{6}'$	5(3)	$\bar{6}' \parallel Z_3$
$6/m$	0	$m \perp Z_3, 6 \parallel Z_3$
$6'/m'$	0	$m' \perp Z_3, 6' \parallel Z_3$
$6/m'$	5(3)	$m' \perp Z_3, 6 \parallel Z_3$
$6'/m$	0	$m \perp Z_3, 6' \parallel Z_3$
622	3(2)	$2 \parallel Z_1, 6 \parallel Z_3$
$6'22'$	0	$2 \parallel Z_1, 6' \parallel Z_3$
$62'2'$	2(1)	$2' \parallel Z_1, 6 \parallel Z_3$
$6mm$	2(1)	$m \perp Z_1, 6 \parallel Z_3$
$6'mm'$	0	$m \perp Z_1, 6' \parallel Z_3$
$6m'm'$	3(2)	$m' \perp Z_1, 6 \parallel Z_3$
$\bar{6}m2$	0	$m \perp Z_1, \bar{6} \parallel Z_3$
$\bar{6}'m'2$	3(2)	$m' \perp Z_1, \bar{6}' \parallel Z_3$
$\bar{6}'m2'$	2(1)	$m \perp Z_1, \bar{6}' \parallel Z_3$
$\bar{6}m'2'$	0	$m' \perp Z_1, \bar{6} \parallel Z_3$
$6/mmm$	0	$m \perp Z_1, m \perp Z_3, 6 \parallel Z_3$
$6'/m'mm'$	0	$m \perp Z_1, m' \perp Z_3, 6' \parallel Z_3$
$6/mm'm'$	0	$m' \perp Z_1, m \perp Z_3, 6 \parallel Z_3$
$6/m'm'm'$	3(2)	$m' \perp Z_1, m' \perp Z_3, 6 \parallel Z_3$
$6/m'mm$	2(1)	$m \perp Z_1, m' \perp Z_3, 6 \parallel Z_3$
$6'/mmm'$	0	$m \perp Z_1, m \perp Z_3, 6' \parallel Z_3$
Cubic		
23	3(1)	$2 \parallel Z_1, 3 \parallel [111]$
$m3$	0	$m \perp Z_1, 3 \parallel [111]$
$m'3$	3(1)	$m' \perp Z_1, 3 \parallel [111]$
432	3(1)	$4 \parallel Z_1, 3 \parallel [111]$
$4'32$	0	$4' \parallel Z_1, 3 \parallel [111]$
$\bar{4}3m$	0	$\bar{4} \parallel Z_1, 3 \parallel [111]$
$\bar{4}'3m'$	3(1)	$\bar{4}' \parallel Z_1, 3 \parallel [111]$
$m3m$	0	$m \perp Z_1, 3 \parallel [111], m \perp [110]$
$m3m'$	0	$m \perp Z_1, 3 \parallel [111], m' \perp [110]$
$m'3m'$	3(1)	$m' \perp Z_1, 3 \parallel [111], m' \perp [110]$
$m'3m$	0	$m' \perp Z_1, 3 \parallel [111], m \perp [110]$

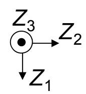

Simple examples

α-Fe (4/*mm'm'*)

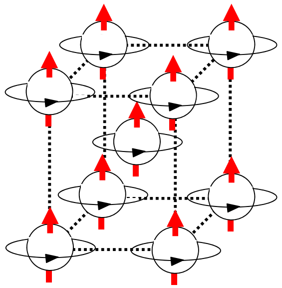

Co (6/*mm'm'*)

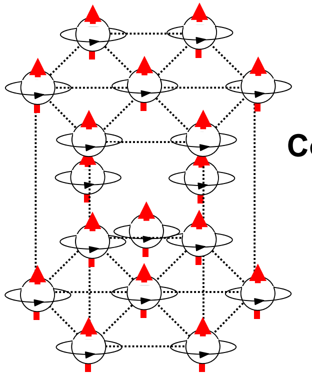

4/mm'm'

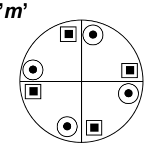

6/mm'm'

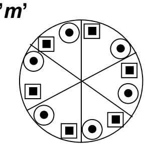

Outline of this lecture

- Symmetry in crystals
- Magnetic symmetry
- Conventional magnetoelectric effect
- Single crystal growth
- Spin-spiral-driven multiferroics
  - Orthorhombic perovskite manganites $RMnO_3$
  - Triangular lattice antiferromagnets
  - Cuprates and ferrites working at room temperature
- Observation of spin-spiral domain structure
- ME effect in magnetically-disordered system

Magnetoelectric effect

Magnetoelectric effect ⇨ Induction of Polarization by Magnetic fields (ME_H)
Induction of Magnetization by Electric fields (ME_E)

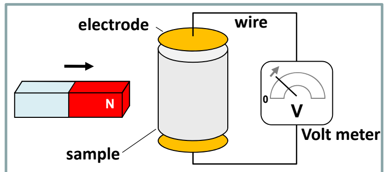

ME_H effect $P_i = \alpha_{ij} H_j$

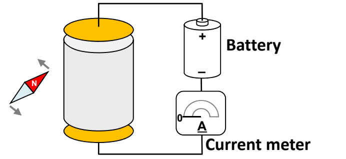

ME_E effect $M_i = \alpha_{ij} E_j$

(P: Electric polarization, a: magnetoelectric coefficient, M: magnetization, H: magnetic field, E:, electric field)

Early history of the ME effect [from "The electrodynamics of magneto-electric media" by T. H. O'Dell]

Researcher [year]	work
P. Curie [1894]	First proposal of the ME effect on symmetry grounds.
Piccard [1924]	Suggests the impossibility of the effect on symmetry grounds.
Debye [1926]	Suggests the effect is impossible.
Van Vleck [1932]	Devotes a section of his book to the reason why no ME effect can exist.
Landau & Lifshitz [1957]	Shows that the ME effect should exist in magnetic crystals.
Dzyaloshinskii [1959]	Shows that the AF Cr_2O_3 has a magnetic symmetry which allows the effect.
Astrov [1960]	First successful observation of the effect in a Cr_2O_3 crystal.

Expansion of free energy of a material in electric (*E*) & magnetic (*H*) fields

$$F = F_0 - \underbrace{\sum_n a_n E^n}_{\vec{P} = -\frac{\partial F}{\partial \vec{E}}} - \underbrace{\sum_n b_n H^n}_{\vec{M} = -\frac{\partial F}{\partial \vec{H}}} - \underbrace{\sum_{m,n} c_{m,n} E^m H^n}_{F_{\text{ME}}} \;\ldots\ldots$$

Electric polarization — Magnetization — Mangetoelectric (ME) effect

$$F_{ME} = -\sum_{i,j=1}^{3} \alpha_{ij} H_i E_j - \sum_{i,j,k=1}^{3} \beta_{ijk} E_i H_j H_k - \sum_{i,j,k=1}^{3} \gamma_{ijk} H_i E_j E_k - \sum_{i,j,k,l=1}^{3} \delta_{ijkl} H_i H_j E_k E_l - \ldots$$

$$\vec{P} = -\frac{\partial F_{ME}}{\partial \vec{E}} \rightarrow P_i = \sum_{j=1}^{3} \alpha_{ij} H_j \quad \text{… Induction of } P \text{ by } H \;(\text{ME}_H \text{ effect})$$

$$\vec{M} = -\frac{\partial F_{ME}}{\partial \vec{H}} \rightarrow M_j = \sum_{i=1}^{3} \alpha_{ij} E_i \quad \text{… Induction of } M \text{ by } E \;(\text{ME}_E \text{ effect})$$

1st order ME effect

Requirements of the 1st order ME effect → **Both space inversion symmetry & time reversal symmetry must be broken.**

Why both *I* and *R* must be broken for 1st order ME effect?

Even function for $\vec{r}$
Odd function for t

$$\vec{P} = A\ \vec{H}$$

Odd function for $\vec{r}$
Even function for t

Which parity does ME tensor A have with respect to $\vec{r}$ and t?

$$\vec{P} = A\ \vec{H} \quad \cdots ①$$

System which I is preserved i.e. which have I in symmetry operation $IA \rightarrow A$	System which R is preserved i.e which have R in symmetry operation $RA \rightarrow A$
By applying I to both sides in ①	By applying R to both sides in ①
$I\vec{P} = I\left(A\vec{H}\right)$	$R\vec{P} = R\left(A\vec{H}\right)$
$\Leftrightarrow I\vec{P} = (IA)\left(I\vec{H}\right)$	$\Leftrightarrow R\vec{P} = (RA)\left(R\vec{H}\right)$
$\Leftrightarrow -\vec{P} = A\vec{H} \cdots ②$	$\Leftrightarrow \vec{P} = A\left(-\vec{H}\right) \cdots ③$
From ① & ② $A \equiv 0$	From ① & ③ $A \equiv 0$

Thus, both *I* & *R* must be broken to have a finite *A*.

Axial tensor properties

Several properties change sign
when the axial system changes from right-handed to left-handed.
(e.g. pyromagnetism, Hall effect …)

⇩

Axial tensors ⟶ depends on handedness

Axial tensors transform in the following manner,

$$T'_{ijk\ldots} = |a| a_{il} a_{jm} a_{kn} \ldots T_{lmn\ldots},$$

↑ Determinant of the direction cosines matrix

|a| = +1 or -1 depending on whether or not the handedness of the axial system changes during transformation

For mirror or inversion symmetry operations, |a| =-1 i.e. the sign of the tensor coefficient changes.

Magnetoelectricity ⟶ ***a second rank axial tensor properties***

$$M_i = \alpha_{ij} E_j$$

M_i is linearly proportional to the applied electric field E_j through the magnetoelectric coefficients Q_{ij}.

Since E is a polar first rank tensor & M is an axial first rank tensor,
the magnetoelectric effect is **an axial second rank tensor** which transforms as follows.

$$M'_i = \pm|a| a_{ij} M_j = \pm|a| a_{ij} \alpha_{jk} E_k$$
$$= \pm|a| a_{ij} \alpha_{jk} a_{lk} E'_l = \alpha'_{il} E'_l \quad ⇨ \quad \alpha'_{il} = \pm|a| a_{ij} \alpha_{jk} a_{lk}$$

In matrix form, the linear magnetoelectric effect transforms in a similar way in going from the old system to the new system.

$$(M') = \pm|a|\ (a)\ (M) = \pm|a|\ (a)\ (\alpha)\ (E)$$
$$= \pm|a|\ (a)\ (\alpha)(a)_t\ (E') = (\alpha')\ (E') \quad ⇨ \quad (\alpha') = \pm|a|\ (a)(\alpha)(a)_t$$

The ME effect vanishes for all symmetry groups containing time reversal symmetry (1').

$$(\alpha') = (-1)(+1)(+1)(\alpha)(+1) = (-\alpha) = (\alpha) = 0$$

The ME effect also disappears for ordinary inversion symmetry ($\bar{1}$) *operations.*

$$(\alpha') = (+1)(-1)(-1)(\alpha)(-1) = (-\alpha) = (\alpha) = 0$$

For space inversion accompanied by time inversion ($\bar{1}'$)*, the ME effect is permitted.*

$$(\alpha') = (-1)(-1)(-1)(\alpha)(-1) = (\alpha) = (\alpha)$$

First magnetoelectric material: Cr_2O_3

Crystal structure: corundum (=Al_2O_3)

Antiferromagnet with T_N =307 K

Magnetic point group: $\bar{3}'m'$

Generating elements

$m' \perp Z_1$, $\bar{3}' // Z_3$

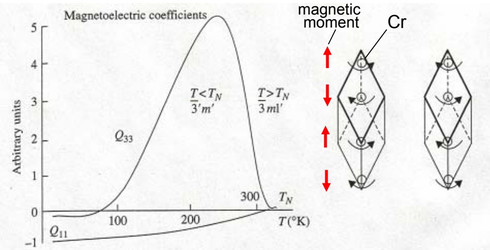

$m' \perp Z_1$

Time reversal

Handedness change by mirror

$$\begin{pmatrix} Q'_{11} & Q'_{12} & Q'_{13} \\ Q'_{21} & Q'_{22} & Q'_{23} \\ Q'_{31} & Q'_{32} & Q'_{33} \end{pmatrix} = (-1)(-1)\begin{pmatrix} -1 & 0 & 0 \\ 0 & 1 & 0 \\ 0 & 0 & 1 \end{pmatrix}\begin{pmatrix} Q_{11} & Q_{12} & Q_{13} \\ Q_{21} & Q_{22} & Q_{23} \\ Q_{31} & Q_{32} & Q_{33} \end{pmatrix}\begin{pmatrix} -1 & 0 & 0 \\ 0 & 1 & 0 \\ 0 & 0 & 1 \end{pmatrix} = \begin{pmatrix} Q_{11} & -Q_{12} & -Q_{13} \\ -Q_{21} & Q_{22} & Q_{23} \\ -Q_{31} & Q_{32} & Q_{33} \end{pmatrix} = \begin{pmatrix} Q_{11} & Q_{12} & Q_{13} \\ Q_{21} & Q_{22} & Q_{23} \\ Q_{31} & Q_{32} & Q_{33} \end{pmatrix}$$

This equality can be satisfied if $Q_{12} = Q_{13} = Q_{21} = Q_{31} = 0$ $\longrightarrow$ $\begin{pmatrix} Q_{11} & 0 & 0 \\ 0 & Q_{22} & Q_{23} \\ 0 & Q_{32} & Q_{33} \end{pmatrix}$

Cr_2O_3

$\bar{3}' // Z_3$

Time reversal

Handedness change by inversion

$$\begin{pmatrix} Q'_{11} & Q'_{12} & Q'_{13} \\ Q'_{21} & Q'_{22} & Q'_{23} \\ Q'_{31} & Q'_{32} & Q'_{33} \end{pmatrix} = (-1)(-1)\begin{pmatrix} 1/2 & -\sqrt{3}/2 & 0 \\ \sqrt{3}/2 & 1/2 & 0 \\ 0 & 0 & -1 \end{pmatrix}\begin{pmatrix} Q_{11} & 0 & 0 \\ 0 & Q_{22} & Q_{23} \\ 0 & Q_{32} & Q_{33} \end{pmatrix}\begin{pmatrix} 1/2 & \sqrt{3}/2 & 0 \\ -\sqrt{3}/2 & 1/2 & 0 \\ 0 & 0 & -1 \end{pmatrix}$$

$$= \begin{pmatrix} (1/4Q_{11}+3/4Q_{22}) & (-\sqrt{3}/4Q_{11}+\sqrt{3}/4Q_{22}) & (\sqrt{3}/2Q_{23}) \\ (\sqrt{3}/4Q_{11}-\sqrt{3}/4Q_{22}) & (3/4Q_{11}+1/4Q_{22}) & (-1/2Q_{23}) \\ (\sqrt{3}/2Q_{32}) & (-1/2Q_{32}) & (Q_{33}) \end{pmatrix}$$

$$= \begin{pmatrix} Q_{11} & 0 & 0 \\ 0 & Q_{22} & Q_{23} \\ 0 & Q_{32} & Q_{33} \end{pmatrix}$$

This equality can be satisfied if $Q_{11} = Q_{22}$ & $Q_{23} = Q_{32} = 0$

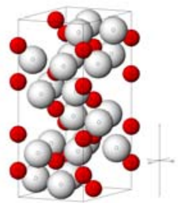

Therefore the magnetoelectric matrix for point group $\bar{3}'m'$ is

$$\begin{pmatrix} Q_{11} & 0 & 0 \\ 0 & Q_{11} & 0 \\ 0 & 0 & Q_{33} \end{pmatrix}$$

Magnetoelectric matrices for the magnetic point groups

$1, \bar{1}'$	$\begin{pmatrix} Q_{11} & Q_{12} & Q_{13} \\ Q_{21} & Q_{22} & Q_{23} \\ Q_{31} & Q_{32} & Q_{33} \end{pmatrix}$	$4', \bar{4}, 4'/m'$	$\begin{pmatrix} Q_{11} & Q_{12} & 0 \\ Q_{12} & -Q_{11} & 0 \\ 0 & 0 & 0 \end{pmatrix}$
$2, m', 2/m'$	$\begin{pmatrix} Q_{11} & 0 & Q_{13} \\ 0 & Q_{22} & 0 \\ Q_{31} & 0 & Q_{33} \end{pmatrix}$	$32, 3m', \bar{3}'m', 422, 4m'm', \bar{4}'2m', 4/m'm'm', 622, 6m'm', \bar{6}'m'2, 6/m'm'm'$	$\begin{pmatrix} Q_{11} & 0 & 0 \\ 0 & Q_{11} & 0 \\ 0 & 0 & Q_{33} \end{pmatrix}$
$2', m, 2'/m$	$\begin{pmatrix} 0 & Q_{12} & 0 \\ Q_{21} & 0 & Q_{23} \\ 0 & Q_{32} & 0 \end{pmatrix}$	$4'22, 4'mm', \bar{4}2m, \bar{4}2'm', 4'/m'mm'$	$\begin{pmatrix} Q_{11} & 0 & 0 \\ 0 & -Q_{11} & 0 \\ 0 & 0 & 0 \end{pmatrix}$
$222, m'm'2, m'm'm'$	$\begin{pmatrix} Q_{11} & 0 & 0 \\ 0 & Q_{22} & 0 \\ 0 & 0 & Q_{33} \end{pmatrix}$	$32', 3m, \bar{3}'m, 42'2', 4mm, \bar{4}'2'm, 4/m'mm, 62'2', 6mm, \bar{6}'m2', 6/m'mm$	$\begin{pmatrix} 0 & Q_{12} & 0 \\ -Q_{12} & 0 & 0 \\ 0 & 0 & 0 \end{pmatrix}$
$22'2', 2mm, m'm2', m'mm$	$\begin{pmatrix} 0 & 0 & 0 \\ 0 & 0 & Q_{23} \\ 0 & Q_{32} & 0 \end{pmatrix}$	$23, m'3, 432, \bar{4}'3m', m'3m'$	$\begin{pmatrix} Q_{11} & 0 & 0 \\ 0 & Q_{11} & 0 \\ 0 & 0 & Q_{11} \end{pmatrix}$
$3, \bar{3}', 4, \bar{4}', 4/m', 6, \bar{6}', 6/m'$	$\begin{pmatrix} Q_{11} & Q_{12} & 0 \\ -Q_{12} & Q_{11} & 0 \\ 0 & 0 & Q_{33} \end{pmatrix}$	Other magnetic groups	$\begin{pmatrix} 0 & 0 & 0 \\ 0 & 0 & 0 \\ 0 & 0 & 0 \end{pmatrix}$

Only 58 magnetic point groups are magnetoelectric.

Polarization (Magnetization) induced by Magnetic (Electric) fields is restricted to magnetic symmetry.

Example; Magnetic symmetry and ME tensor in $GaFeO_3$ (Remeikite)

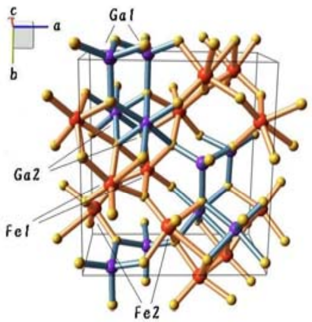

・Characteristic of crystal structure

4 sub-cells in a unit cell

In each sub-cell,

3 $(Fe,Ga)O_6$ octahedra (Ga2,Fe1,Fe2)

1 GaO_4 tetrahedron (Ga1)

→breaking space inversion sym. *I*

・space group: $Pc2_1n$

・ferrimagnetic (spontaneous polarization //*c*)

→breaking time reversal sym. *R*

$$m'2'm \rightarrow \{1, RIC_{2a}, RC_{2b}, IC_{2c}\}$$

by applying these symmetry operations $\rightarrow A = \begin{pmatrix} 0 & 0 & 0 \\ 0 & 0 & \alpha_{23} \\ 0 & \alpha_{32} & 0 \end{pmatrix}$

to $\vec{P} = A\vec{H}$

ME_H effect in conventional magnetoelectrics

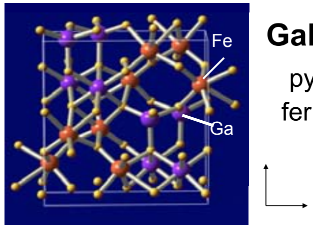

$GaFeO_3$

pyroelectric
ferrimagnetic

m'2'm

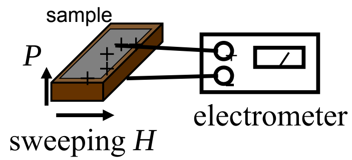

$$P = Q H$$

↓ t differential

current, Charge, Electrode area

$$\frac{I}{S} = \frac{1}{S}\frac{dQ}{dt} = \frac{dP}{dt} = Q\frac{dH}{dt}$$

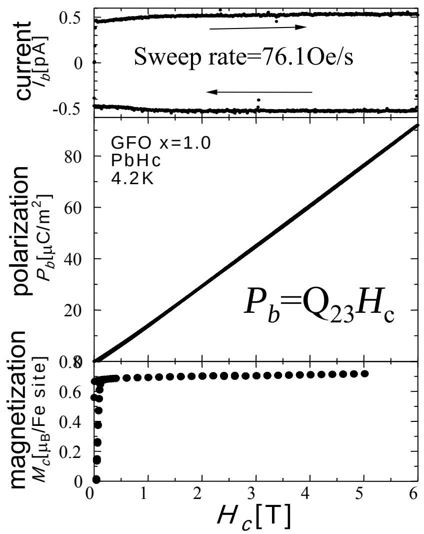

System with breaking of either *I* & *R*

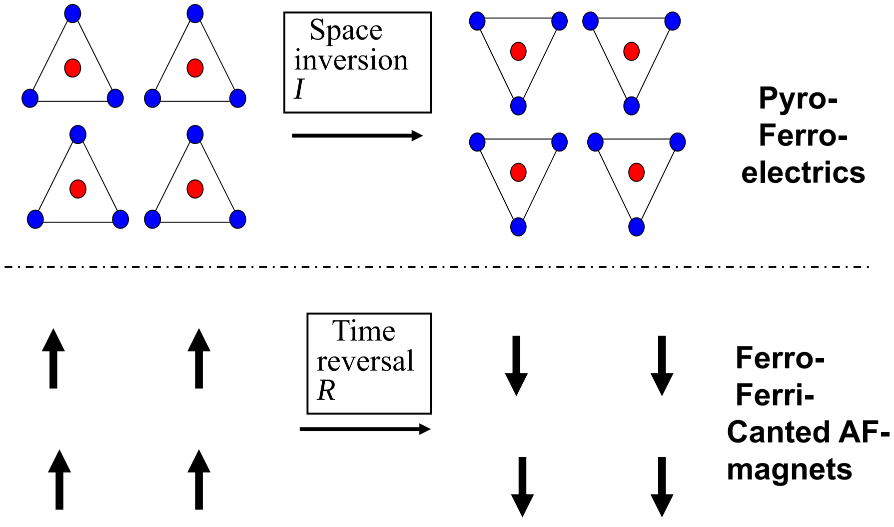

System with breaking of both *I* & *R*

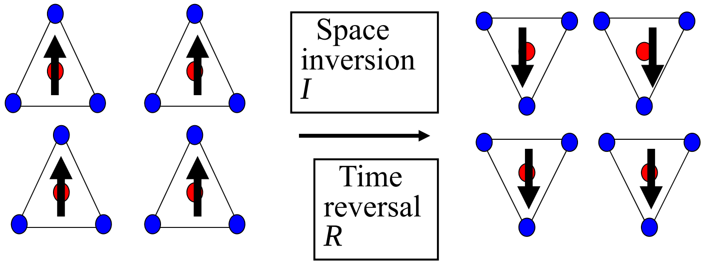

⇩

Magnetoelectric Multiferroics

Important remarks by former studies

In a magnetically ordered compound, magnetic symmetry (not fundamental crystal symmetry) determines its ferroelectric property.

In noncollinear spiral spin structure, magnetic symmetry operations are quite different from crystallographic one.

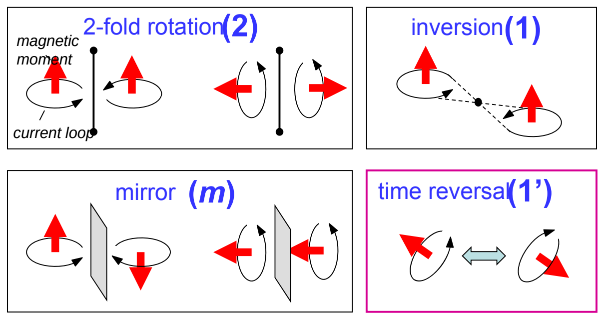

reference **Properties of Materials: Anisotropy, Symmetry, Structure**
by Robert E. Newnham, Oxford University Press (2005).

Outline of this lecture

- Symmetry in crystals
- Magnetic symmetry
- Conventional magnetoelectric effect
- Single crystal growth
- Spin-spiral-driven multiferroics
  - Orthorhombic perovskite manganites *R*MnO_3
  - Cuprates and ferrites working at room temperature
- Observation of spin-spiral domain structure
- ME effect in magnetically-disordered system

Single crystal growth for inorganic materials

•Directional Solidification/Bridgeman Method
•Flux Method
•Czochralski growth
•Floating Zone Method
•Chemical vapor transport method

They enable growth of materials which melt congruently, and those that do not, and require a flux.


Pt crucibles


Furnaces


Crystals collection grown by J. P. Remeika (Bell Labs.)

$MnWO_4$

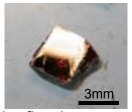

by floating zone


by flux

$CuCrO_2$

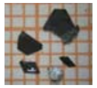
Flux: $CuO + K_2Cr_2O_7$

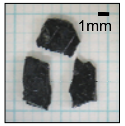

Flux: Bi_2O_3

Importance of phase diagram to grow single crystals

"Phase Diagrams for Ceramists" American Chemical Society

Example: Phase diagram of Fe_2O_3-$YFeO_3$

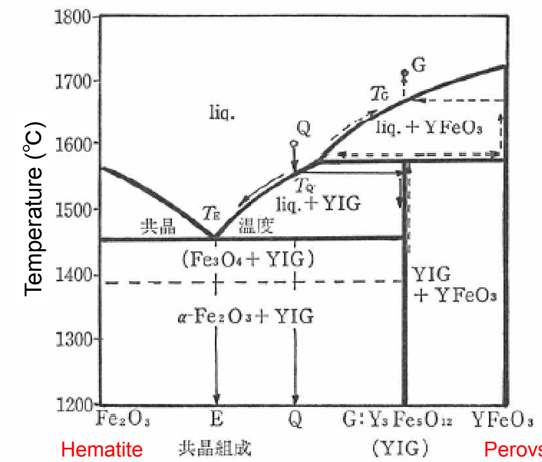

Hematite Y-ion garnet Perovskite

Floating zone (FZ) method

The basic idea in float zone (FZ) crystal growth is to move a liquid zone through the material. If properly seeded, a single crystal may result.

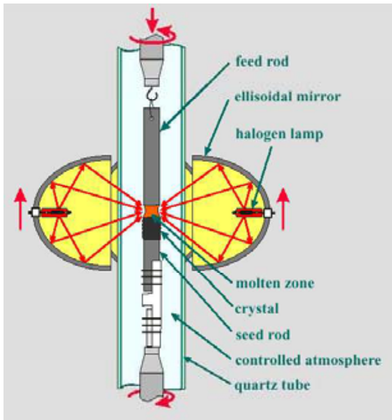

From
http://people.seas.harvard.edu/~jones/es154/lectures/lecture_2/materials/materials.html

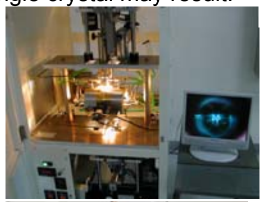

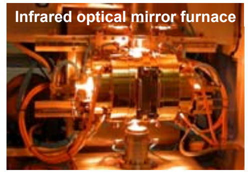
Infrared optical mirror furnace

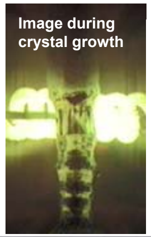
Image during crystal growth


$DyVO_4$ grown by FZ method

Traveling solvent floating zone (FZ) method

An effective method to grow compounds which melt incongruently.

Growth of a high-T_c cuprate, $(La,Sr)_2CuO_4$

Phase diagram of La_2O_3-CuO

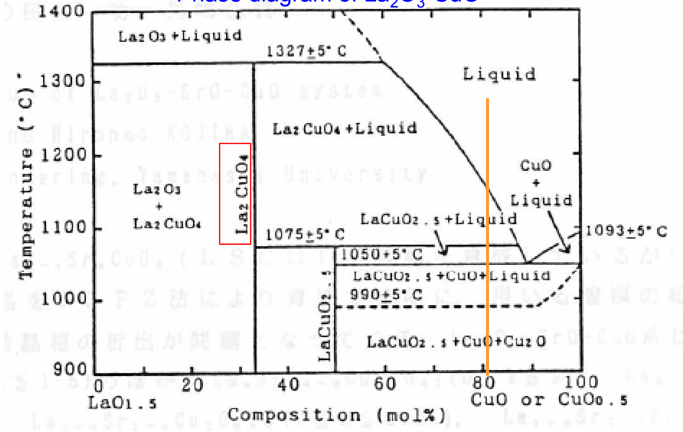

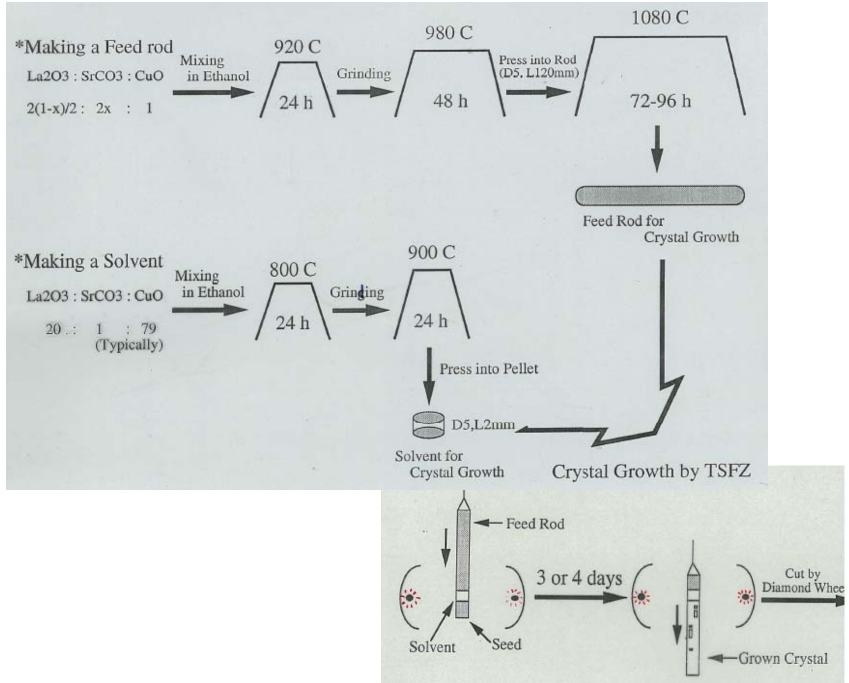

When the solid state reaction could not stabilize the formation of the focused phase,

*** change the pressure.**

*** change the oxygen partial pressure.**

$BiMnO_3$

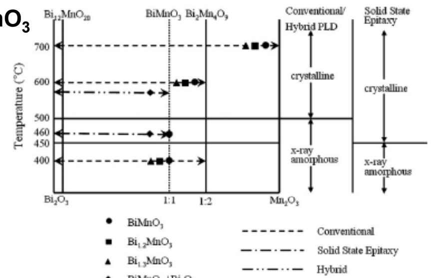

Havelia et al., JAP 106, 123509 (2009)

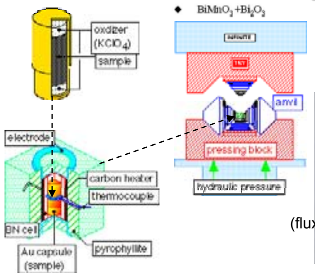

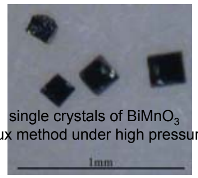

single crystals of $BiMnO_3$ (flux method under high pressure)

CuO

Phase diagram of Cu- O system

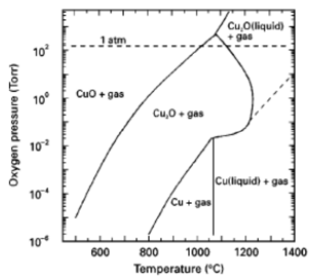

Applying~10 atm O_2 pressure makes the growth of CuO crystal.

CuO grown by by FZ method.

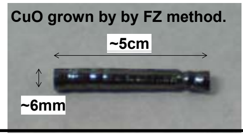

Outline of this lecture

- Symmetry in crystals
- Magnetic symmetry
- Conventional magnetoelectric effect
- Single crystal growth
- Spin-spiral-driven multiferroics
  - Orthorhombic perovskite manganites $RMnO_3$
  - Cuprates and ferrites working at room temperature

- Observation of spin-spiral domain structure
- ME effect in magnetically-disordered system

Classification of magnetoelectric multiferroics

Origins to induce polar structure in multiferroics

$^*6s^2$ lone pair of Bi or Pb (Seshadri & Hill Chem. Mat. 2001)

Bi^{3+} or Pb^{2+} ion with two electrons on the 6s lone pair ($[Xe]4f^{14}5d^{10}6s^2$) that moves away from the centrosymmetric position in its oxygen surrounding (as in $PbTiO_3$).

$Pb(A,B)O_3$ (A=Fe, Mn, Co…; B=W, Nb…) [T_C(FE)~300~400K T_N(M)~100~200K]
$BiFeO_3$ [T_C(FE)~1123K T_N(M)~650K], $BiMnO_3$ [T_C(FE)~773K T_C(M)~110K]

***Geometric ferroelectrics** (van Aken et al. Nature Mat. 2004)

An electric dipole moment is induced by a nonlinear coupling to nonpolar lattice distortions, such as the buckling of Y–O planes and tilts of manganese–oxygen bipyramids

Hexagonal $RMnO_3$ (R=Y, Ho, etc.) [T_C(FE)~900K T_N(M)~100K]

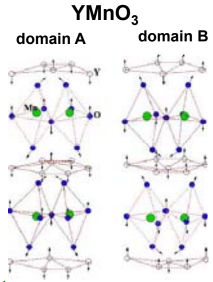

***Charge ordering** (Efremov et al, Nat, Mater. 2004, Ikeda et al. Nature 2005, Tokunaga et al. Nature Mat. 2006)

$LuFe_2O_4$, $(Pr,Ca)_3Mn_2O_7$

**Origins of magnetic and ferroelectric ordering are independent. (Their ferroelectric order often appears at higher temperature than magnetic one.)*

***Ferroelectricity induced by magnetic order**

Classification of magnetically-induced polarization

Cluster model composed of two transition metal ions link by ligand ion

C. Jia et al., PRB 74, 224444 (2006); PRB 76, 144424 (2007).

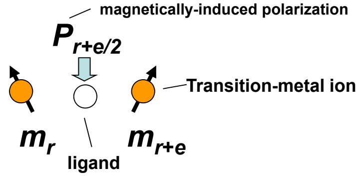

$$P_{r+e/2} = P^{MS}(m_r\cdot m_{r+e})e + P^{SP} e\times(m_r\times m_{r+e}) + P^{ORB}[(e\cdot m_r)m_r-(e\cdot m_{r+e})m_{r+e}]$$

1. term from exchange striction (Chapon et al. PRL 2006, Sergenko et al. PRL 2006)
   RMn_2O_5 (R=Tb, Dy, Y, Ho, …)
   Ca_3CoMnO_6
   $GdFeO_3$

2. term from spin current (Katsura et al. PRL 2005, Harris PRL 2005, Mostovoy PRL 2006)
   $TbMnO_3$
   $Ni_3V_2O_8$
   $MnWO_4$

3. term from variation of p-d hybridization (Jia et al. PRB 2006, Arima JPSJ 2007)
   $Cu(Fe,Al)O_2$, $CuCrO_2$

Ferroelectricity induced by exchange striction ($\sim J\, S_i\cdot S_j$)

Cr_2O_3

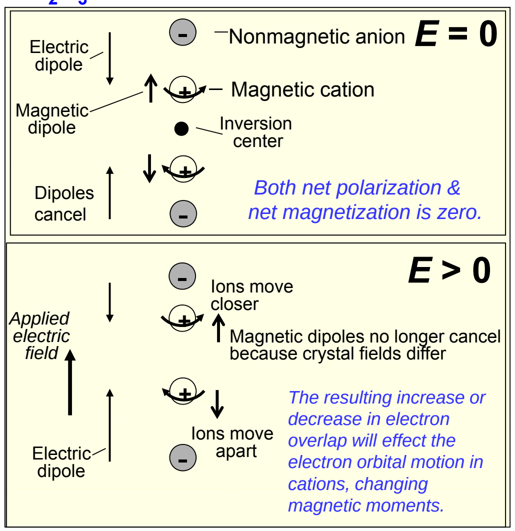

J. Phys. Soc. Japan **16** (1961) 2589

Origin of Magnetoelectric Effect in Cr_2O_3

By Muneyuki Date, Junjiro Kanamori, and Masashi Tachiki

Department of Physics, Osaka University, Nakanoshima, Osaka

(Received September 26, 1961)

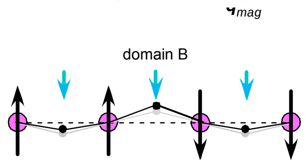

Gray and black circles represent oxygen ions in paramagnetic and magnetically ordered phases.

Ca_3CoMnO_6
Choi et al. PRL 100, 047601 (2008)
$DyFeO_3$, $GdFeO_3$
Tokunaka et al. PRL 100, 047601 (2008)
Tokunaga et al. Nat. Mat. 8, 558 (2009).

Classification of magnetically-induced polarization

Cluster model composed of two transition metal ions link by ligand ion

C. Jia et al., PRB 74, 224444 (2006); PRB 76, 144424 (2007).

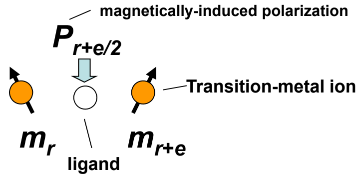

$$P_{r+e/2} = P^{MS}(m_r\cdot m_{r+e})e + P^{SP} e\times(m_r\times m_{r+e}) + P^{ORB}[(e\cdot m_r)m_r-(e\cdot m_{r+e})m_{r+e}]$$

1. term from exchange striction (Chapon et al. PRL 2006, Sergenko et al. PRL 2006)
   RMn_2O_5 (R=Tb, Dy, Y, Ho, …)
   Ca_3CoMnO_6
   $GdFeO_3$

2. term from spin current (Katsura et al. PRL 2005, Harris PRL 2005, Mostovoy PRL 2006)
   $TbMnO_3$
   $Ni_3V_2O_8$
   $MnWO_4$

3. term from variation of p-d hybridization (Jia et al. PRB 2006, Arima JPSJ 2007)
   $Cu(Fe,Al)O_2$, $CuCrO_2$

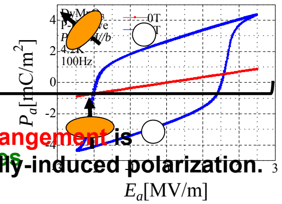

Noncollinear spiral spin arrangement is a key for magnetically-induced polarization.

Remarkable magnetic field effects on electric properties

Spin spiral mechanism for multiferroics

Ferroelectricity induced
by a spiral magnetic order
that breaks the inversion symmetry.

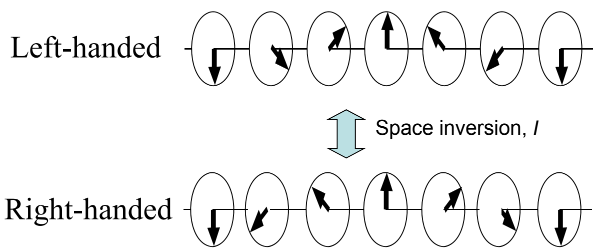

The origin of such ferroelectricity is driven by magnetism.

Magnetoelectric effect in Screw Spiral

Siratori & Kita, JPSJ 48, 1443 (1980)

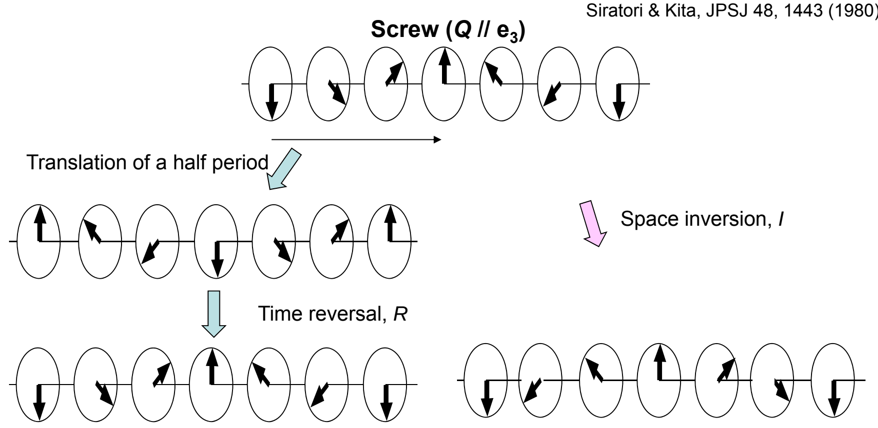

λ/2 translation + time reversal *R*
symmetry operation

Space inversion *I*
NOT symmetry operation

In screw structure, only *I* is broken. ⇨ **1st order ME tensor vanishes, But 2nd order ME tensor does exist.**

$$M_i = \gamma_{ijk} H_j E_k$$

Classification of modulated spin structures

Cox, Takei, & Shirane, J. Phys. Chem. Solids 24, 405 (1963).

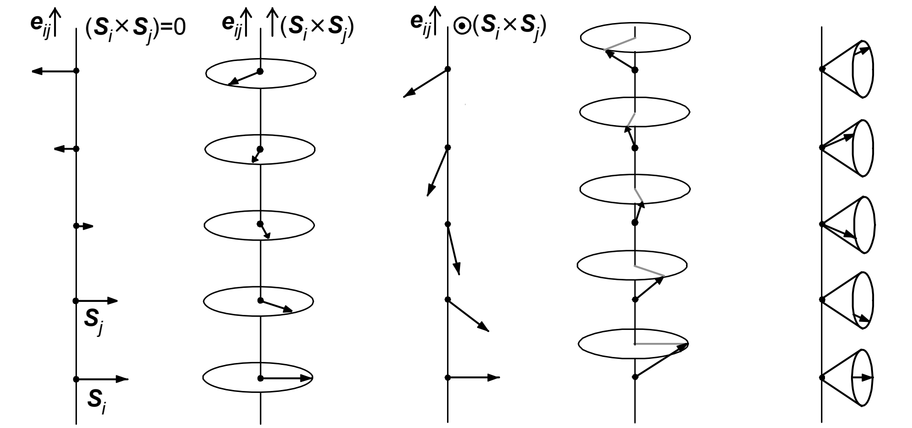

(a) Sinusoid (b) Screw (c) Cycloid (d) Cone [I] (e) Cone [II]

Former works studying the magnetoelectric coupling in systems with spiral spin structures

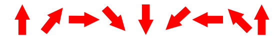

Cr_2BeO_4 [$T_{C(FE)}$~27K]

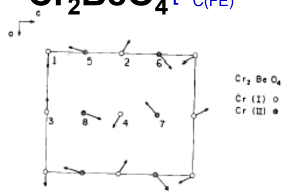

D. E. Cox et al.
JAP 40, 1124 (1969)

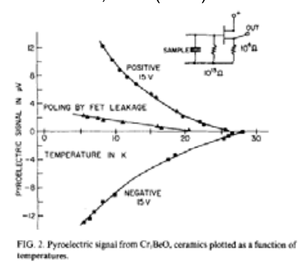

FIG. 2. Pyroelectric signal from Cr_2BeO_4 ceramics plotted as a function of temperatures.

R. E. Newnham et al.
JAP 49, 6088 (1979)

$ZnCr_2Se_4$ [$T_{C(FE)}$~20K]

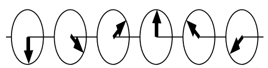

Screw spin along <100>

J. Akimitsu et al.
JPSJ 44, 172 (1978)

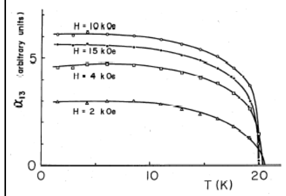

K. Shiratori & E. Kita
JPSJ 48, 1443 (1980)

RMn_2O_5 [$T_{C(FE)}$~37K]

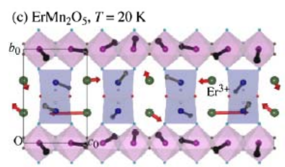

H. Kimura, Y. Noda et al., JPSJ 76, 074706 (2007).

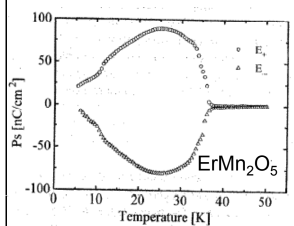

Y. Koyata & K. Kohn,
Ferroelectrics 204, 115 (1997)

Control of spin helicity by magnetoelectric cooling process & its detection by polarized neutron diffraction

JOURNAL OF THE PHYSICAL SOCIETY OF JAPAN, Vol. 48, No. 4, APRIL, 1980

A Method of Controlling the Sense of the Screw Spin Structure

Kiiti SIRATORI, Jun AKIMITSU,† Eiji KITA and Masakazu NISHI††

$ZnCr_2Se_4$

Considering the magnetic symmetry of a screw spin structure, it was shown that the sense of the screw spin structure can be controlled by a magnetoelectric cooling. It was confirmed experimentally in $ZnCr_2Se_4$ by means of a polarized neutron diffraction.

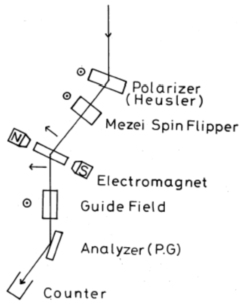

Polarization dependence of $0,0,k_0$ reflection after ME cooling

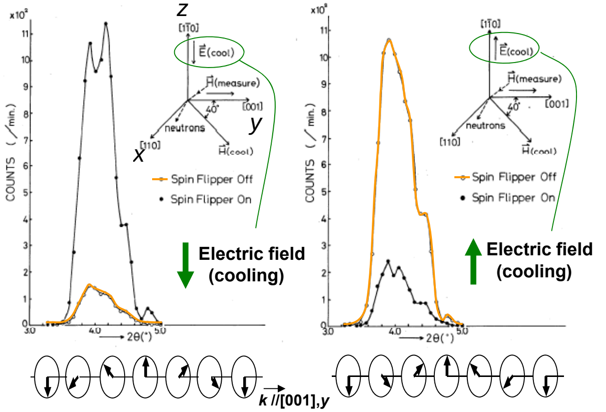

Breaking space inversion symmetry in spiral spin systems

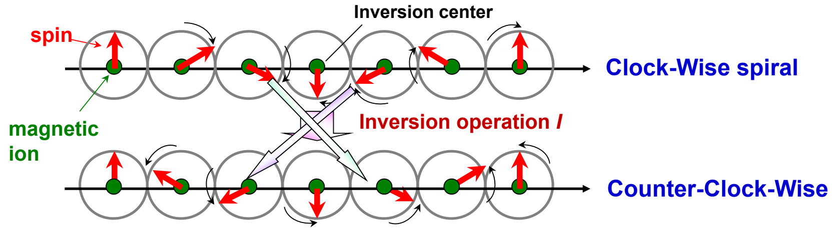

The CW & CCW spiral structures are inverted by *I* to each other. However, these two spiral structures are not identical.

Thus, the inversion symmetry is broken by a spiral spin order.

To make system ferroelectric,

1. Cycloidal spiral structure

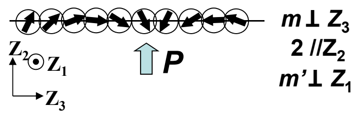

2. Screw spiral structure + low crystal symmetry

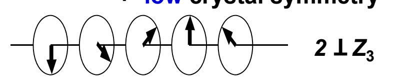

e.g., monoclinic 2/*m* (non-polar) → Removal of *I* → monoclinic 2 (polar)

Materials design

How to produce the spiral magnetic structure

Competing magnetic interactions

An approach to exploring new magnetoelectric multiferroics

We focus on magnetic insulators with competing magnetic interactions (spin frustration) as candidates of new multiferroics.

Normal antiferromagnet

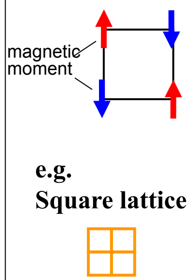

e.g. Square lattice

Geometrical spin frustration

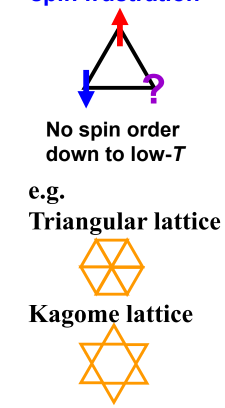

No spin order down to low-*T*

e.g. Triangular lattice

Kagome lattice

Quasi-spin frustration

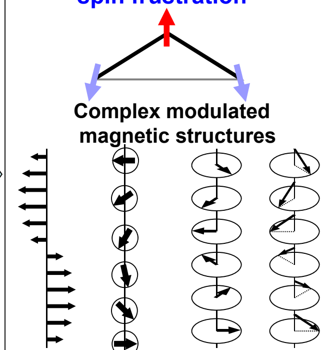

List of spin-spiral-driven ferroelectrics

Compound	Crystal structure	Magnetic ion	Proposed spin structure	Temperature range (K)	Ref.
$RMnO_3$ (R=Tb, etc.)	O (mmm) [perovskite]	Mn^{3+} S=2	cycloidal	≤ 28	Kimura *et al.* (2003)
$Ni_3V_2O_8$	O (mmm)	Ni^{2+} S=1	cycloidal	3.9~6.3	Lawes *et al.* (2005)
$(Ba,Sr)_2M_2Fe_{12}O_{22}$	R (-3m) [haxaferrite]	Fe^{3+} S=5/2	screw, L-conical (B=0) T-conical (B>0)	≤ ~110	Kimura *et al.* (2005)
$CuFeO_2$	R -3m [delafossite]	Fe^{3+} S=5/2	collinear(B=0) screw (B>0)	≤ 11	Kimura *et al.* (2005)
$CoCr_2O_4$	C ($m3m$) [spinel]	Co^{2+} Cr^{3+} S=3/2 S=3/2	T-conical	≤ 26	Yamasaki *et al.* (2006)
$MnWO_4$	M (2/m) [walframite]	Mn^{2+} S=5/2	cycloidal	7~12.5	Taniguchi *et al.* (2006)
$RbFe(MoO_4)_2$	R (-3m)	Fe^{3+} S=5/2	screw	≤ 3.8	Kenzelmann *et al.* (2006)
$LiCu_2O_2$	O (mmm)	Cu^{2+} S=1/2	cycloidal	≤ 23	Park *et al.* (2007)
$LiCuVO_4$	O (mmm)	Cu^{2+} S=1/2	cycloidal	≤ 2.4	Naito *et al.* (2007)
CuO	M (2/m) [tenorite]	Cu^{2+} S=1/2	cycloidal + screw	212~230	Kimura *et al.* (2008)
$ACrO_2$ (A=Ag, Cu)	R (-3m) [delafossite]	Cr^{3+} S=3/2	screw	≤ 24	Seki *et al.* (2008)
$FeVO_4$	Tri (-1)	Fe^{3+} S=5/2	cycloidal	≤ 16	Daoud-Aladine *et al.* (2009)
$CuCl_2$	M (2/m) [distorted CdI_2]	Mn^{2+} S=5/2	cycloidal	≤ 24	Seki *et al.* (2010)
Mn_2GeO_4	O (mmm) [olivine]	Mn^{2+}	cycloidal	<5.5	White et al. (2012)

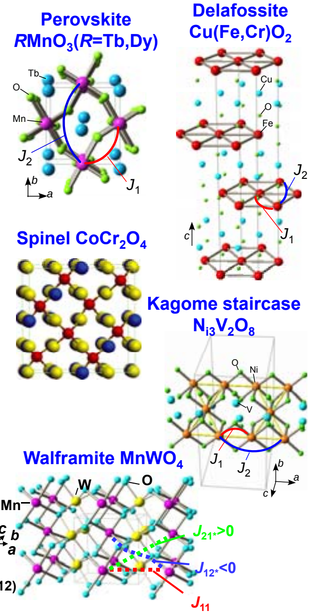

Outline of this lecture

- Symmetry in crystals
- Magnetic symmetry
- Conventional magnetoelectric effect
- Single crystal growth
- Spin-spiral-driven multiferroics
  - Orthorhombic perovskite manganites $RMnO_3$
  - Cuprates and ferrites working at room temperature

- Observation of spin-spiral domain structure
- ME effect in magnetically-disordered system

Change in lattice distortion in $RMnO_3$ (all of them are *Pbnm* orthorhombic)

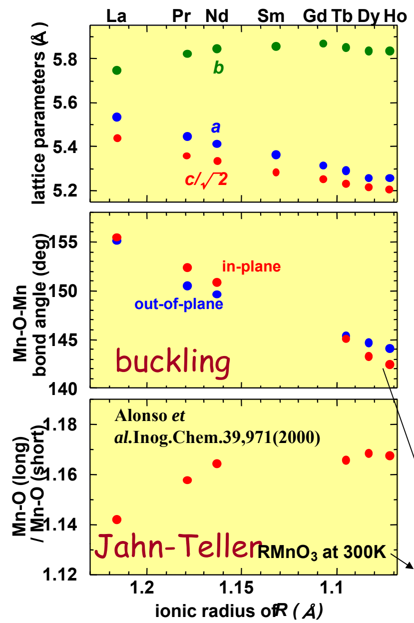

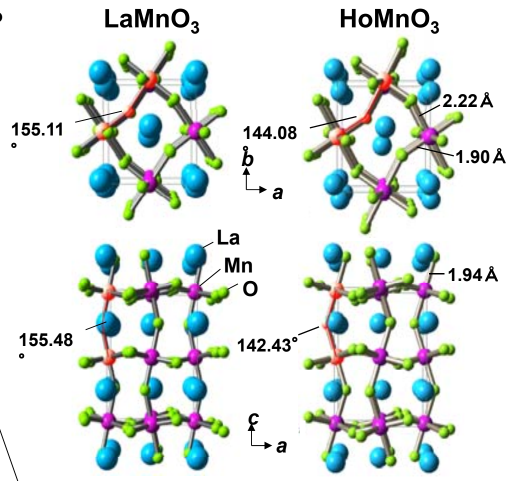

With decrease of ionic radius of R

1. Mn-O-Mn bond angle drastically decreases.
2. JT-distortion slightly increases.

Complex phase diagram & variety of phases in perovskite manganites $RMnO_3$

Kimura et al.
PRB 68, 060403(R) (2003)

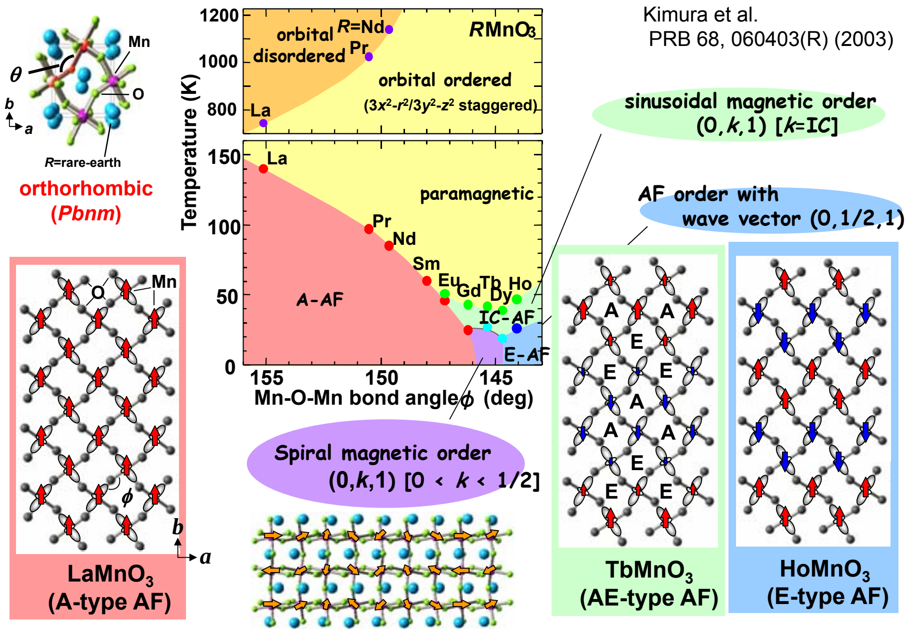

Competing magnetic interactions in $RMnO_3$

MnO_2 plane in perovskite manganite

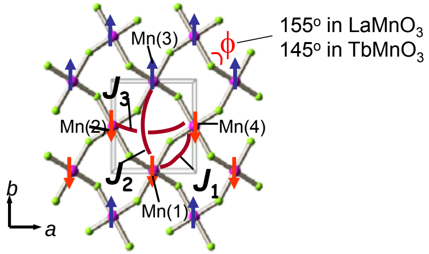

Kimura, Ishihara et al. PRB 68, 060403(R) (2003)

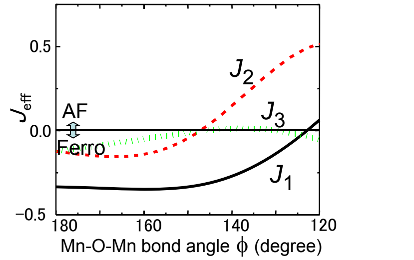

Competition between *FM Nearest-Neighbor* & *AF Next-Nearest-Neighbor* interactions

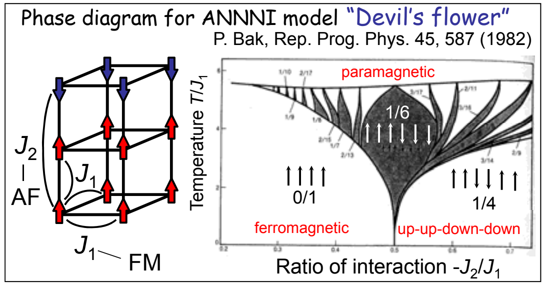

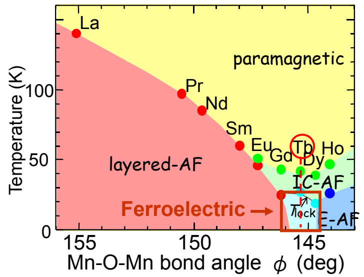

Ferroelectric order accompanied by spiral magnetic order in $TbMnO_3$

T. Kimura *et al*. Nature 426, 55 (2003).

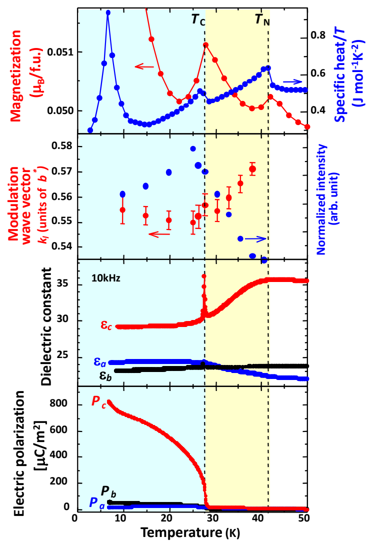

Spin structure model of $TbMnO_3$

M. Kenzelmann et al. PRL 95, 087206 (2005).
T. Arima et al., PRL 96, 097202 (2006).

at $T < T_C(E)$

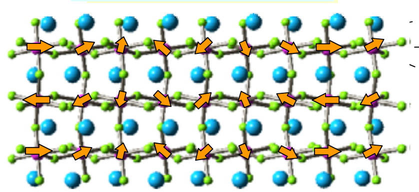

Sinusoidal spin structure

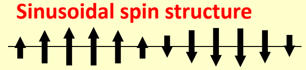

Spiral spin structure

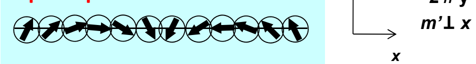

Ferroelectricity induced by exchange striction (~$J S_i \cdot S_j$)

Sergienko et al. PRL 97, 227204 (2006)
Picozzi et al., PRL 99, 227201 (2007).

$TmMnO_3$

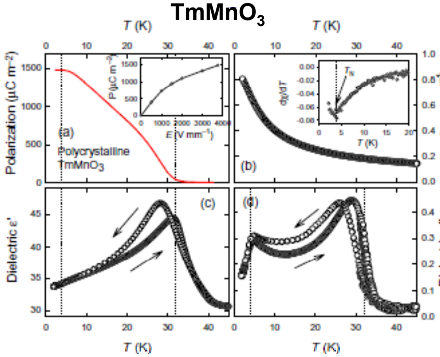

Pomjakushin et al.
New. J. Phys.PRB 11, 043019 (2010)

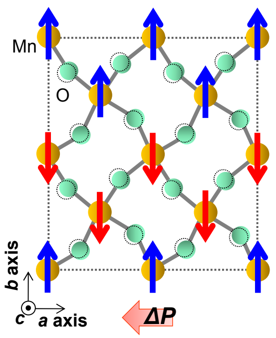

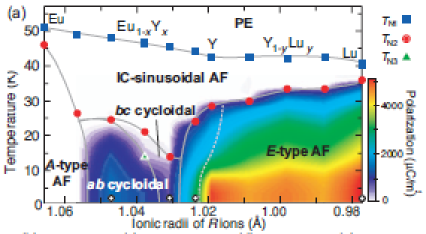

Ishiwata et al. PRB 81, 100411(R) (2010)

Large ME effects near the phase boundary in $TbMnO_3$, $DyMnO_3$

T. Kimura *et al*. Nature 426, 55 (2003).

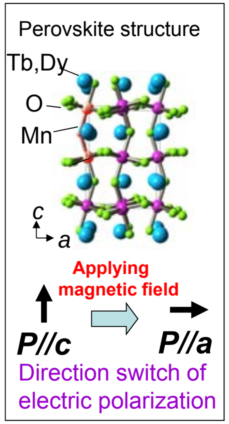

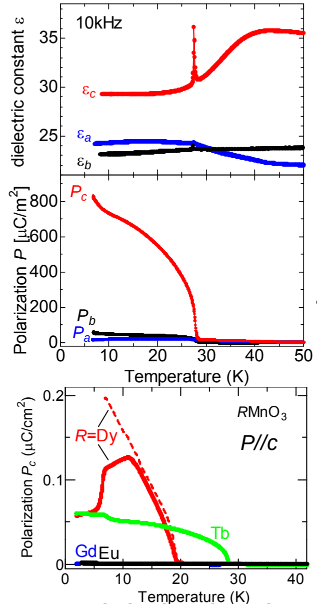

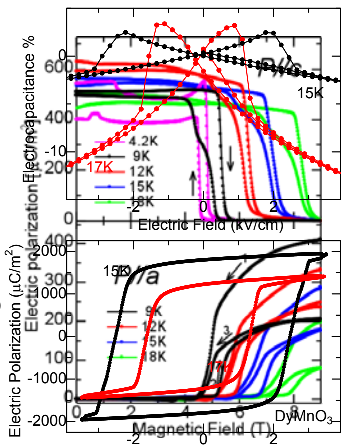

Magnetically-controllable ferroelectric properties

Ferroelectricity with spontaneous polarization along the *c*-axis

Outline of this lecture

- Symmetry in crystals
- Magnetic symmetry
- Conventional magnetoelectric effect
- Single crystal growth
- Spin-spiral-driven multiferroics
  - Orthorhombic perovskite manganites $RMnO_3$
  - Cuprates and ferrites working at room temperature
- Observation of spin-spiral domain structure
- ME effect in magnetically-disordered system

Spin frustration often suppresses magnetic ordering temperature.

Most of induced-multiferroics only operate below ~40 K.

How to obtain induced-ferreoelectrics with high-T_C?

1. Low dimensional cuprates with Cu^{2+}

Variation of superexchange interaction J in several undoped cuprates

Mizuno, Tohyama, Maekawa et al. PRB 57, 5326 (1998); Shimizu et al. JPSJ 72, 2165 (2003), etc.

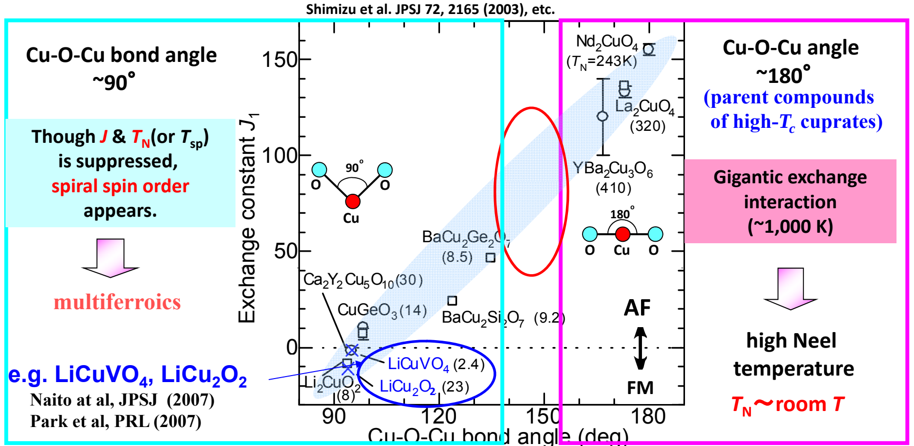

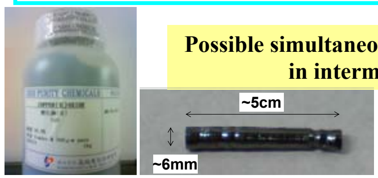

Possible simultaneous occurrence of spin-spiral & high T_N in intermediate Cu-O-Cu bond angle

Tenorite CuO (Cu–O–Cu bond angle 146°)

Crystal & magnetic structures of CuO

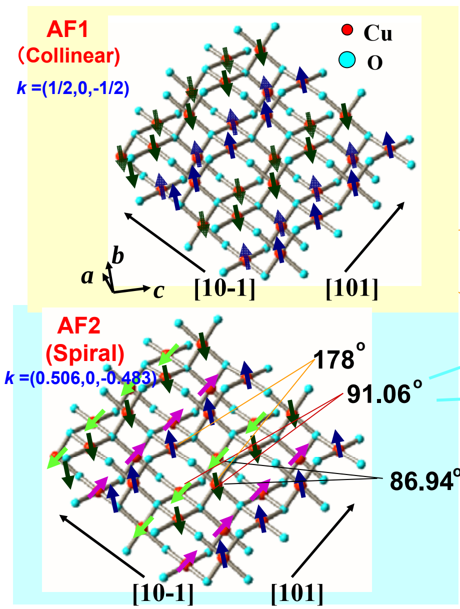

M. Ain et al., J. Phys.: Condens. Matter 4, 5327 (1992).

Successive phase transitions

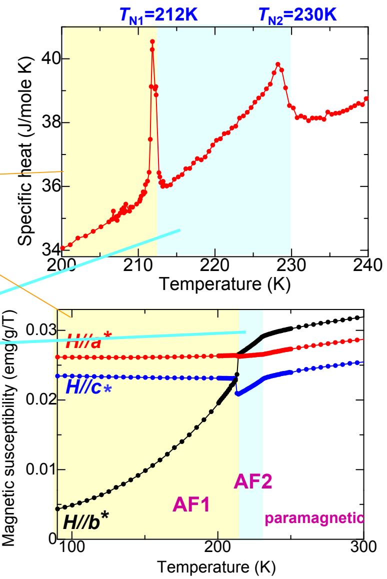

Ferroelectricity with *P//b*-axis in spin spiral phase of CuO

Kimura et al., Nature Mater. 7, 291 (2008).

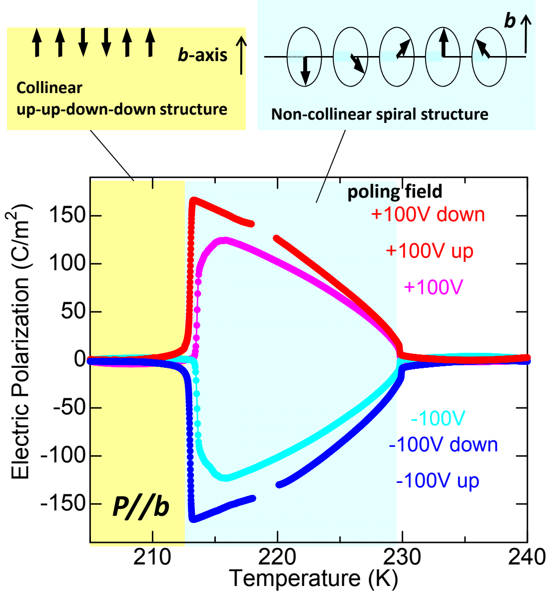

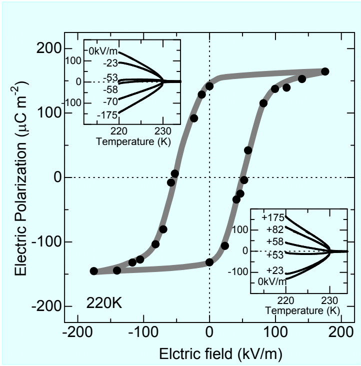

Spiral-induced ferroelectricity with T_C=230 K

Magnetic-field effect on ferroelectricity in CuO

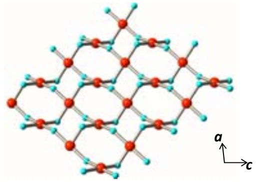

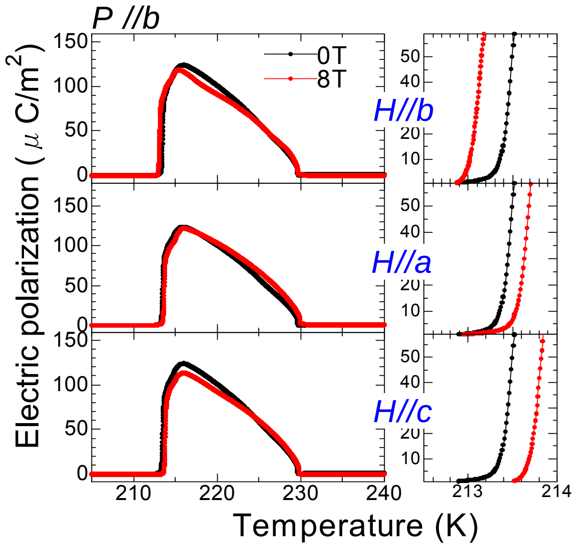

Unfortunately, the effect of *H* on ferroelectricity was quite small in CuO.

Spin frustration often suppresses magnetic ordering temperature.

Most of induced-multiferroics only operate below ~40 K.

How to obtain induced-ferreoelectrics with high-T_C?

1. Low dimensional cuprates with Cu^{2+}

2. Iron oxides with hexagonal structure (hexaferrites)

Refrigerator magnet

Magnetoelectric Y-type hexaferrite $(Ba,Sr)_2Me_2Fe_{12}O_{22}$ (*Me*=Zn, Mg, etc.)

Kimura et al., PRL. 94, 137201 (2005)

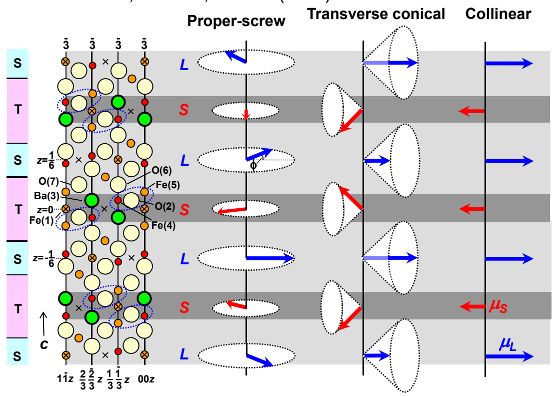

Momozawa et al., JPSJ 54, 771 (1985).

Ishiwata et al., PRB 81, 174418 (2010).

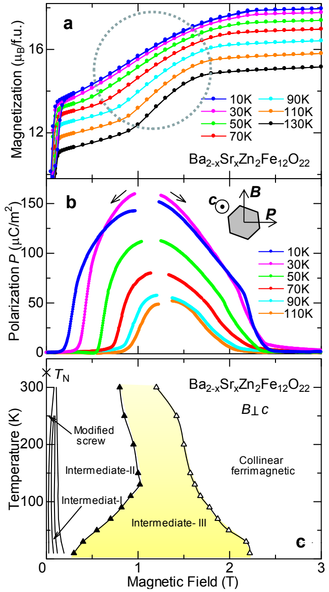

Ferroelectric intermediate-III phase survives up to near room temperature.

Transverse conical spiral spin order can induce *P* via the spin-current mechanism.

However, suppression of resistivity does not allow experimental observation of polarization above ~110K.

Low-Magnetic-Field Control of Electric Polarization in Y-type hexaferrites $(Ba,Sr)_2Me_2Fe_{12}O_{24}$

$Ba_2Mg_2Fe_{12}O_{22}$
Ishiwata et al. Science 319, 1643 (2008).

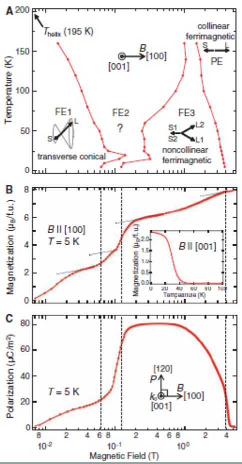

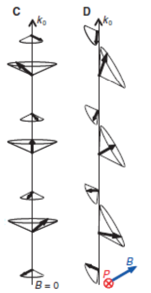

$Ba_{0.5}Sr_{1.5}Zn_2(Fe,Al)_{12}O_{22}$
Chun et al. PRL 104, 037204 (2010).

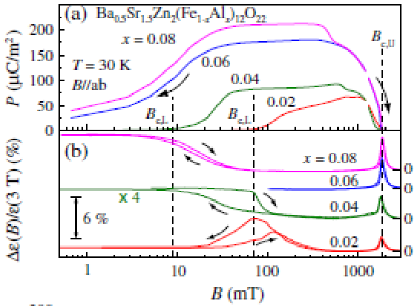

ME effects can be observed by low H (~mT) but only at low T (<~30K).

We pursue **room-temperature magnetoelectrics** in other types of hexaferrites.

Hexaferrite showing
1. *a spiral magnetic order above room temperature*
2. *highly insulating electric property at room temperature*

Classification of hexagonal ferrites (hexaferrites) - chemical formula -

J. Smit & H.P.J. Wijn, Ferrite (Philips' Technical Library, 1959)

a=5.9(Å)

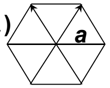

M-type (magnetoplumbite)
$BaFe_{12}O_{19}$
(c=23.19Å)

- W-type : $BaM_2Fe_{16}O_{27}$ (c=32.84Å)
- Y-type : $Ba_2M_2Fe_{12}O_{22}$ (c=43.56Å)
- Z-type : $Ba_3M_2Fe_{24}O_{41}$ (c=52.30Å)
- X-type : $Ba_2M_2Fe_{28}O_{46}$ (c=84.11Å)
- U-type : $Ba_4M_2Fe_{36}O_{60}$ (c=113Å)

(M = divalent metal)

Refrigerator magnet

Classification of hexagonal ferrites
- Stacking sequence composed of 3 types of blocks-

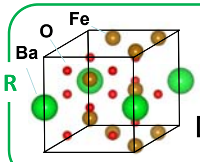

R-block
$[BaFe_6O_{11}]^{2-}$

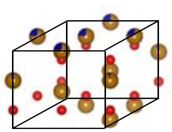

S-block (Spinel)
$M_2^{2+}Fe_4O_8$

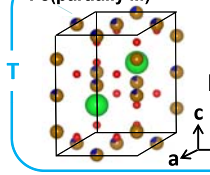

T-block
$Ba_2Fe_8O_{14}$

J. Smit & H.P.J. Wijn, Ferrite (Philips' Technical Library, 1959)

	Chem. form.	stacking	c(Å)	S.G.
M	$BaFe_{12}O_{19}$	RSR*S*	23.19	$P6_3/mmc$
W	$BaM_2Fe_{16}O_{27}$	$RS_2R^*S^*_2$	32.84	$P6_3/mmc$
Y	$Ba_2M_2Fe_{12}O_{22}$	$(TS)_3$	43.56	$R\text{-}3/m$
Z	$Ba_3M_2Fe_{24}O_{41}$	RSTSR*S*T*S*	52.3	$P6_3/mmc$
X	$Ba_2M_2Fe_{28}O_{46}$	$(RSR^*S^*_2)_3$	84.11	$R\text{-}3/m$
U	$Ba_4M_2Fe_{36}O_{60}$	$(RSR^*S^*TS^*)_3$	113	$R\text{-}3/m$

The prime(') and asterisk (*) symbols indicates that the corresponding block is rotated 120° or 180° about the c axis, respectively.

Crystal structures of 6 main types of hexaferrites

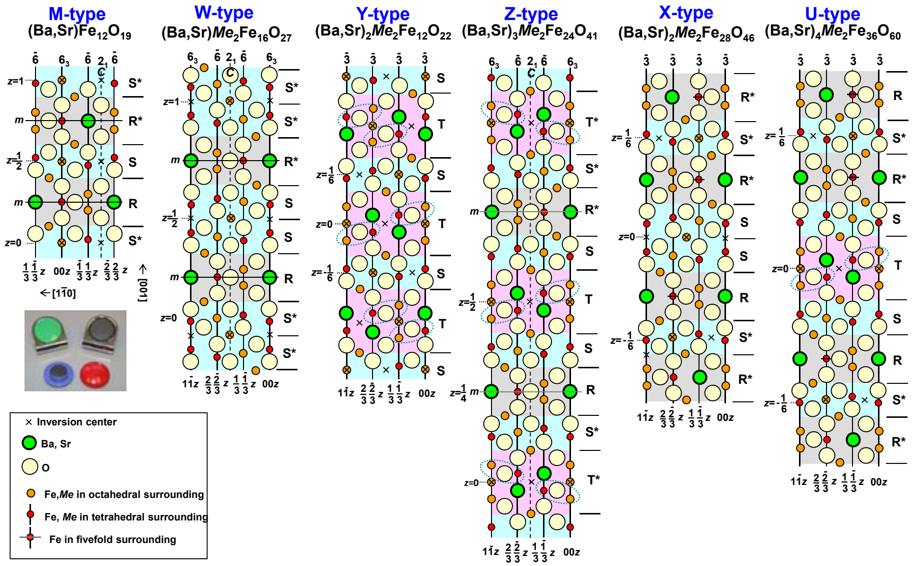

Appearance of noncollinear spiral magnetic order in hexaferrites

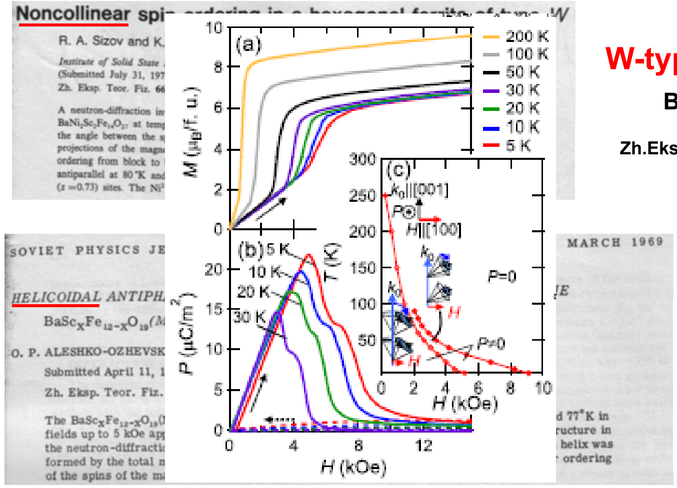

W-type

$BaNi_2Sc_2Fe_{14}O_{27}$

Zh.Eksp. Teor. Fiz. 66, 368 (1974)

M-type

$BaSc_xFe_{12-x}O_{19}$

Zh.Eksp. Teor. Fiz. 55, 820 (1968)

c.f. ME effect in M-type [Tokunaga et al., PRL 105, 257201 (2010).]

Former studies on magnetism of Z-type hexaferrites

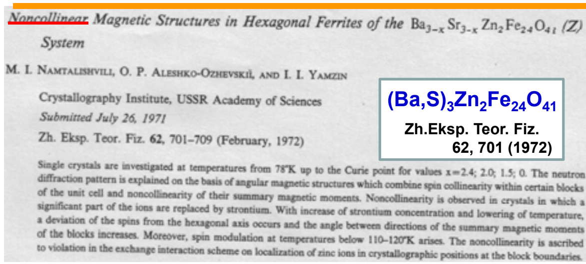

Noncollinear Magnetic Structures in Hexagonal Ferrites of the $Ba_{3-x}Sr_{3-x}Zn_2Fe_{24}O_{41}$ *(Z) System*

M. I. Namtalishvili, O. P. Aleshko-Ozhevskiĭ, and I. I. Yamzin

Crystallography Institute, USSR Academy of Sciences

Submitted July 26, 1971

Zh. Eksp. Teor. Fiz. 62, 701–709 (February, 1972)

Single crystals are investigated at temperatures from 78°K up to the Curie point for values x=2.4; 2.0; 1.5; 0. The neutron diffraction pattern is explained on the basis of angular magnetic structures which combine spin collinearity within certain blocks of the unit cell and noncollinearity of their summary magnetic moments. Noncollinearity is observed in crystals in which a significant part of the ions are replaced by strontium. With increase of strontium concentration and lowering of temperature, a deviation of the spins from the hexagonal axis occurs and the angle between directions of the summary magnetic moments of the blocks increases. Moreover, spin modulation at temperatures below 110–120°K arises. The noncollinearity is ascribed to violation in the exchange interaction scheme on localization of zinc ions in crystallographic positions at the block boundaries.

$(Ba,S)_3Zn_2Fe_{24}O_{41}$

Zh.Eksp. Teor. Fiz. 62, 701 (1972)

Noncollinear spin structure?

Pullar et al., Mater. Res. Bull. 36, 1531 (2001).

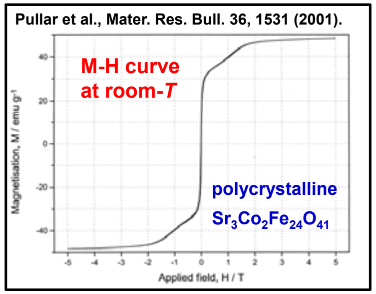

Takada et al., JAP 100, 043904 (2006).

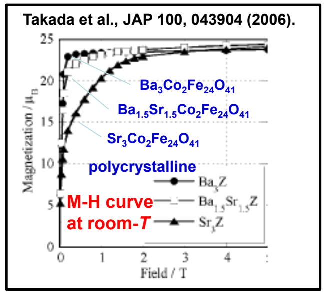

M of $Sr_3Co_2Fe_{24}O_{41}$ increases in a stepwise fashion.

→ Similar to magnetoelectric Y-type hexaferrites

Crystal structures of 6 main types of hexaferrites

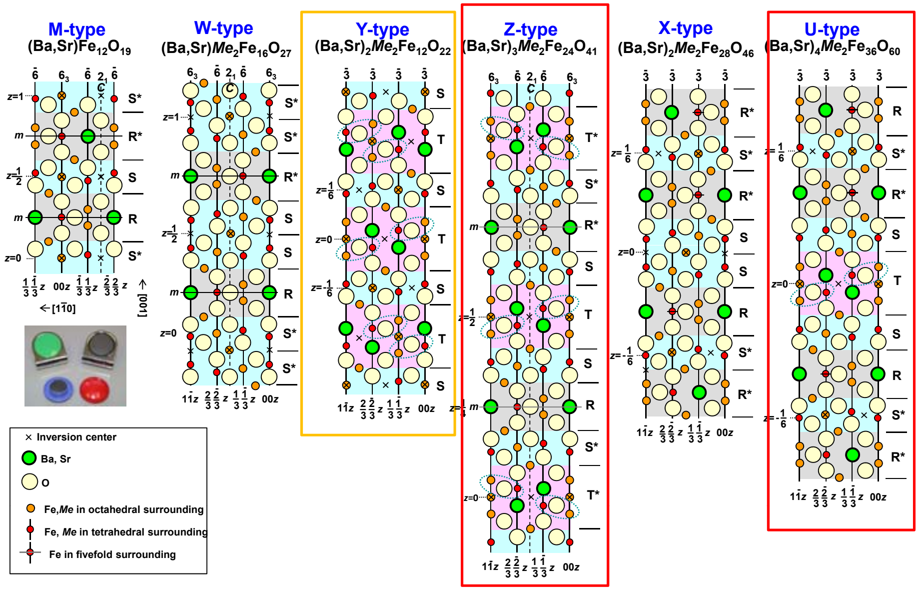

Experimental procedures

*Sample synthesis

Z-type $(Ba,Sr)_3Co_2Fe_{24}O_{41}$ *& U-type* $(Ba,Sr)_4Co_2Fe_{36}O_{60}$ *studied here are polycrystalline samples prepared by the conventional solid-state reaction technique.*

Starting chemicals

$BaCO_3$
$SrCO_3$
Fe_2O_3
Co_3O_4

calcine → 800~1000℃, 16~20h, in air

crush & sinter → 1150-1300℃, 5~50h, in air or O_2 flow

*Measurements

-Powder x-ray diffraction (room temperature)
-Resistivity (room temperature)
-Magnetization (~10K < T < ~800 K)
-Dielectric constant (~10K < T < ~400 K)
-Electric polarization (~10K < T < ~400K)
-Powder neutron diffraction (~10K < T < ~640K)

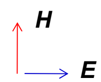

Magnetic fields were applied in a direction normal to electric fields.

Enhancement of Resistivity in Hexaferrites

Y-type

Chai et al., New J. Phys. 11, 073030 (2009).

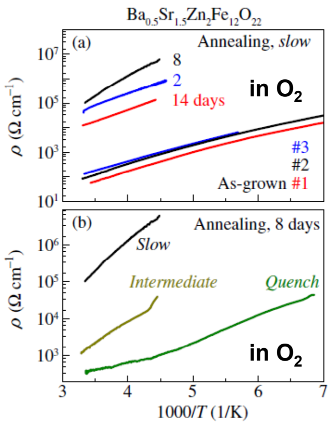

Z-type

$Ba_3Co_2Fe_{24}O_{41}$ $Sr_3Co_2Fe_{24}O_{41}$

Z		BaZ	122	10.8Z	SrZ
Specific	(air)	0.2	0.5	0.4	0.2
Resistivity(O_2) (10^9Ω-cm)		2.2	2.3	1.4	3.9
Tanδ (%)	(air)	7.7	1.8	5.0	20.0
	(O_2)	1.0	0.7	2.0	5.5

The increase of the resistivity for Z-type hexaferrites hot-pressed in oxygen has been reported.

O. Kimura et al, *J. Am. Ceram. Soc.* 78, 2857-2860 (1995).

Evaluation of sample quality (purity, resistivity)

X-ray diffraction patterns

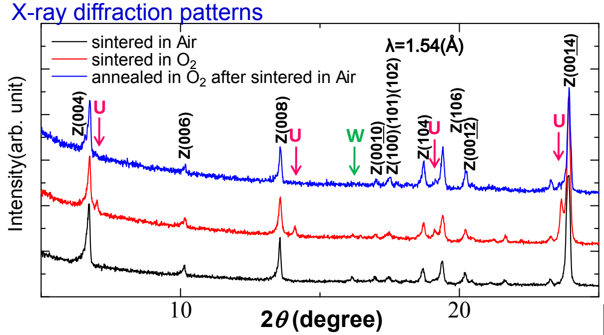

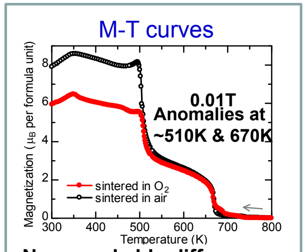

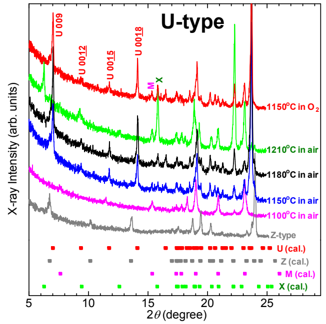

Resistivity at r.t.

atmosphere	impurity	resistivity
Air	W	kΩcm
O_2	U	GΩcm
O_2 anneal		GΩcm

Sample annealed in O_2 after sintered in air shows very high resistivity and includes no impurities.

[100]-zone high-angle annular dark-field scanning TEM (HAADF-STEM) images for two hexaferrite samples

Z-type $(Ba,Sr)_3Me_2Fe_{24}O_{41}$

RSTSR*S*T*S*

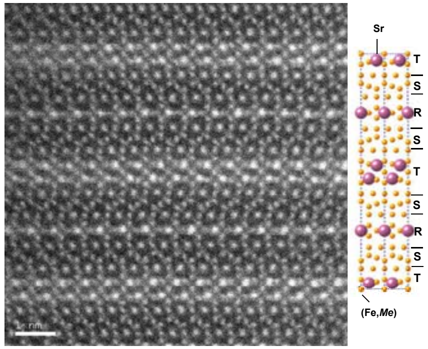

U-type $(Ba,Sr)_4Me_2Fe_{36}O_{60}$

(RSR*S*TS*)$_3$

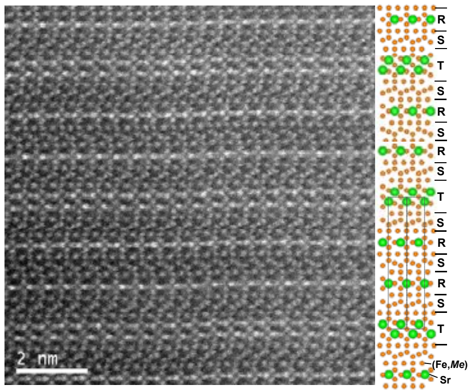

Low field ME effect of Z-type $Sr_3Co_2Fe_{24}O_{41}$ at room temperature

Kitagawa et al., Nature Mater. 9, 797 (2010).

polycrystalline ceramics sintered in oxygen.

✓In the region where magnetization M shows metamagnetic fashion, polarization P can be observed.

⇨ Z-type hexaferrite shows ME effect!!

✓In addition, P can be measured up to 395K.

⇨ Ferroelectric transition temperature T_c is higher than room temperature!!

✓P appears by the application of low magnetic field.

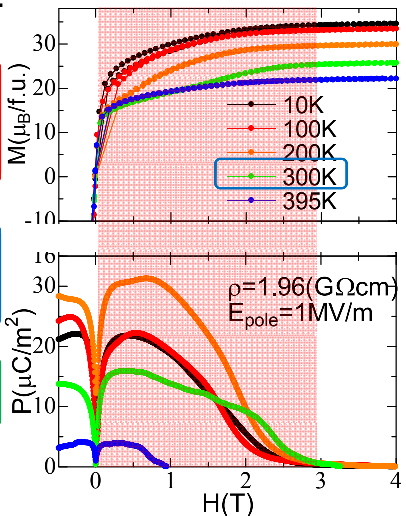

Magnetoelectric effects are observed at a wide temperature range including room temperature.

Room-temperature ME effect of $Sr_3Co_2Fe_{24}O_{41}$

polycrystalline ceramics sintered in oxygen.

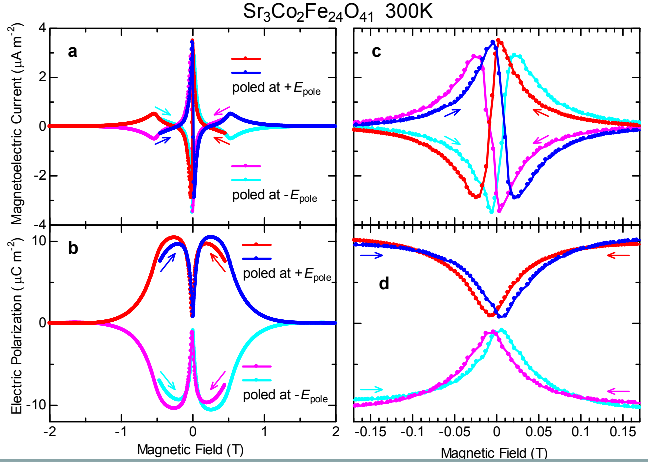

***ME coefficient defined as $\alpha=\mu_0 dP/dB$**

The α exceeds 1×10^{-10} s/m below 0.04T and reached a maximum ~2.5×10^{-10}s/m at 0.003T.

(c.f. α in Cr_2O_3: 4×10^{-12} s/m; α in Z-type single crystal: 3×10^{-9} s/m by Chun arXiv:1111.4525)

Origin of magnetoelectric effect –Neutron diffraction-

Soda et al., PRL 106, 087201 (2011).

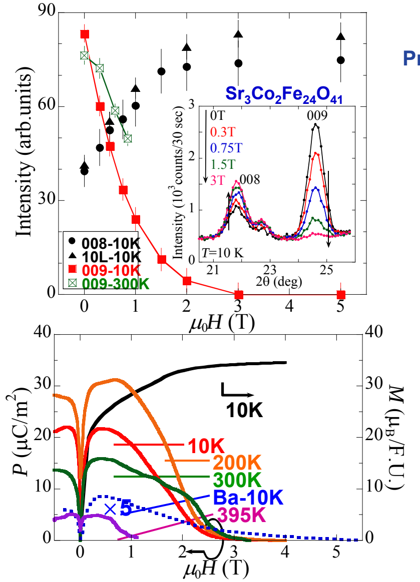

Proposed spin structure related to ME effect in Z-type $Sr_3Co_2Fe_{24}O_{41}$

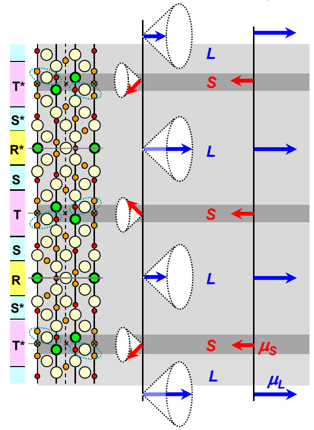

In analogy with Y-type hexaferrites, the r.t. ME effect can be understood in terms of *P* induced by a transverse conical spin structure through the spin-current mechanism.

Non-volatility of reversible polarization

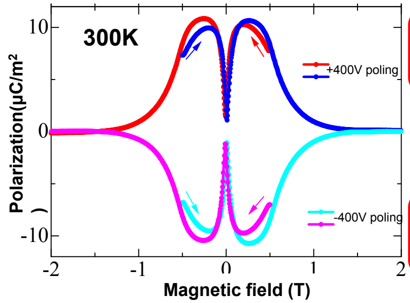

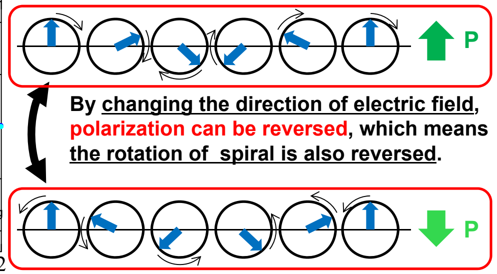

Ferroelectric domains are aligned by electric field (poling).

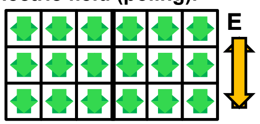

Once sample becomes ferroelectric, polarization is memoried unless sample becoms paraelectric

Magnetism and magnetoelectricity of U-type $Sr_4Co_2Fe_{36}O_{60}$

K. Okumura et al., *APL* 98, 212504 (2011)

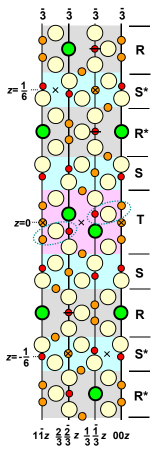

Powder neutron diffraction

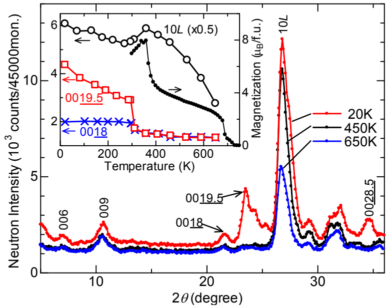

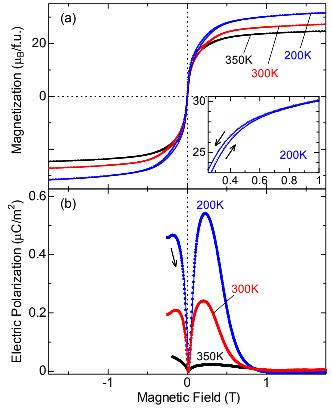

Corresponding to the appearance of the magnetic order with the propagation vector (0,0,3/2), a small magnetoelectric effect was observed below T_{N2} ~350 K.

Summary (magnetoelectric haxaferrites)

Various hexaferrite compounds were highlighted in terms of their high-temperature and low-field magnetoelectric operation.

M-type $(Ba,Sr)Fe_{12}O_{19}$, Y-type $(Ba,Sr)_2\mathit{Me}_2Fe_{12}O_{22}$, Z-type $(Ba,Sr)_3\mathit{Me}_2Fe_{24}O_{41}$, U-type $(Ba,Sr)_4\mathit{Me}_2Fe_{36}O_{60}$

***The ME effect appears even below several hundreds Oe and persists up to ~400 K.**

***The ME effects can be originated from a transverse conical spin structure.**

This result has the promise of ME device applications including non-volatile memory where information is stored as electrically-detectable & -controllable spin-helicity.

Left-handed spin-helicity (0) Right-handed spin-helicity (1)

Outline of this lecture

- Symmetry in crystals
- Magnetic symmetry
- Conventional magnetoelectric effect
- Single crystal growth
- Spin-spiral-driven multiferroics
  - Orthorhombic perovskite manganites $RMnO_3$
  - Cuprates and ferrites working at room temperature
- Observation of spin-spiral domain structure
- ME effect in magnetically-disordered system

by scanning resonant x-ray microdiffraction

with Y. Hiraoka (Osaka), Y. Tanaka (SPring8), S. Shin (SPring8)

Imaging spiral magnetic domains in Ho by circularly polarized Bragg diffraction

J.C. Lang et al., J. Appl. Phys. 95, 6537 (2004)

Ho metal

[spiral magnetic order with $(0,0, L\pm\tau)$ below T_N=133K]

X-ray energy *E*~ 8.071 eV (~ Ho L_3-edge $2p \rightarrow 5d$)

Size of circularly polarized x-ray beam

25 μm × 25μm

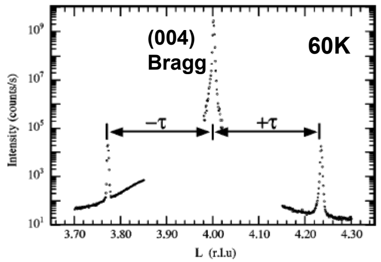

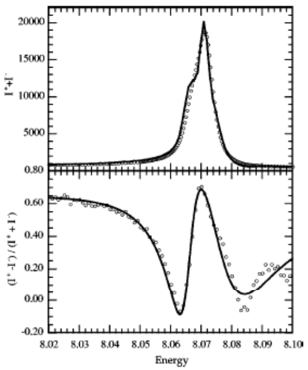

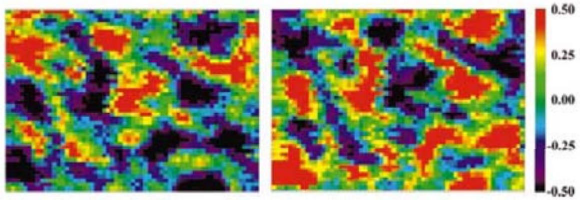

(0.6X0.45mm²)

Imaging spiral magnetic domains in multiferroics by circularly polarized X-ray

$Ni_3V_2O_8$

Fabrizi, Phys. Rev. B **82**, 024434 (2010).

Nonresonant X-ray

Beam size ≈ 380 × 250 μm²

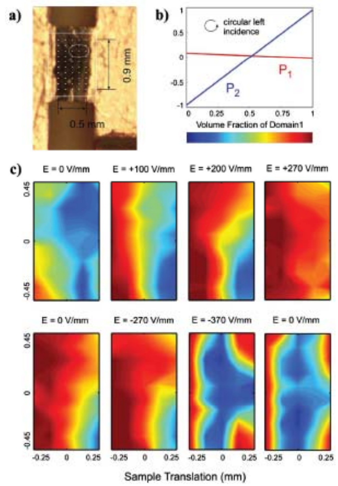

$DyMnO_3$

Schierle, Phys. Rev. Lett. **105**, 167207 (2010).

X-ray energy : Dy M_5-edge

Beam size ≈ 300 × 100 μm²

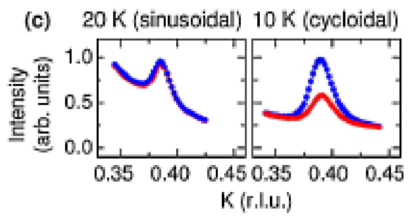

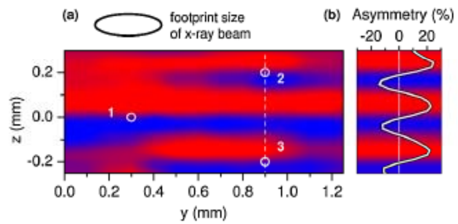

Magnetoelectric Y-type hexaferrite $(Ba,Sr)_2Me_2Fe_{12}O_{22}$ (*Me*=Zn, Mg, etc.)

Kimura et al., PRL. 94, 137201 (2005)

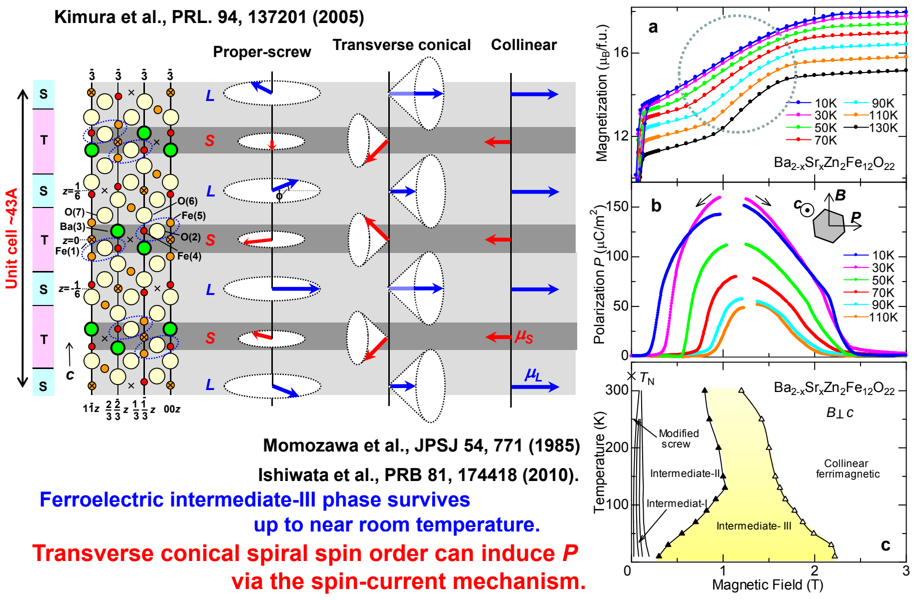

Momozawa et al., JPSJ 54, 771 (1985)

Ishiwata et al., PRB 81, 174418 (2010).

Ferroelectric intermediate-III phase survives up to near room temperature.

Transverse conical spiral spin order can induce *P* via the spin-current mechanism.

Circularly polarized x-ray diffraction study of $Ba_{0.8}Sr_{1.2}Zn_2Fe_{12}O_{22}$

Mulders et al., PRB 81, 092405 (2010).

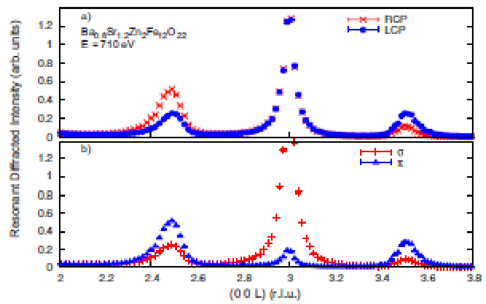

Magnetic diffraction intensity along *c*

$$I_{right} \propto \left(\cos^2\theta + \frac{1}{2}\sin^2 2\theta \mp \chi\cos\theta\, s\right.$$

$$I_{left} \propto \left(\cos^2\theta + \frac{1}{2}\sin^2 2\theta \pm \chi\cos\theta\, s\right.$$

F_{11}, F_{1-1} : atomic prope

q (= k_i - k_f), *G* : reciproc

If the fractions of the right- and left-handed spin-chiral domains are *a* and (1-*a*), respectively

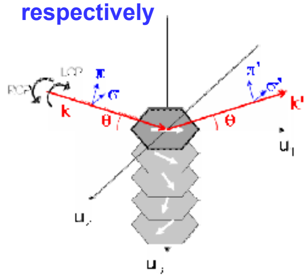

$$I_a^{(-)} \Big/ I_a^{(+)} = \frac{\cos^2\theta + \frac{1}{2}\sin^2 2\theta \mp (1-2a)\cos\theta\sin 2\theta}{\cos^2\theta + \frac{1}{2}\sin^2 2\theta \pm (1-2a)\cos\theta\sin 2\theta}$$

Incident polarization	(003^-) Exp.	(003^-) Calc.	(003^+) Exp.	(003^+) Calc.
RCP	0.50	0.52	0.11	0.10
LCP	0.24	0.25	0.25	0.23

***a* = 0.77**

Imaging spin-chiral domains in $Ba_{0.5}Sr_{1.5}Zn_2Fe_{12}O_{22}$ by circularly polarized X-ray

Sample $Ba_{0.5}Sr_{1.5}Zn_2Fe_{12}O_{22}$ T_N ~ 310 K magnetic satellite (0,0,3*n*±ε)

Experimental conditions (@BL17SU, Spring-8)

Incident x-ray energy 710 eV

Illuminated sample area 60 x 15 μm²
with a 25 μm step

Penetration depth ~40 nm

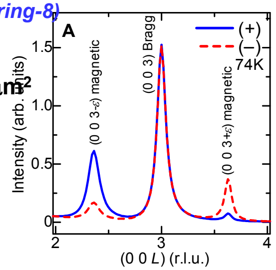

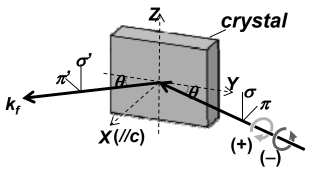

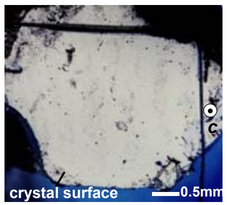

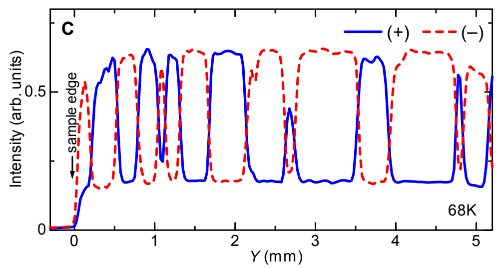

Spatial images of spin-chiral domain structure in $Ba_{0.5}Sr_{1.5}Zn_2Fe_{12}O_{22}$ at 68 K

Hiraoka et al., PRB 84, 064418 (2011).

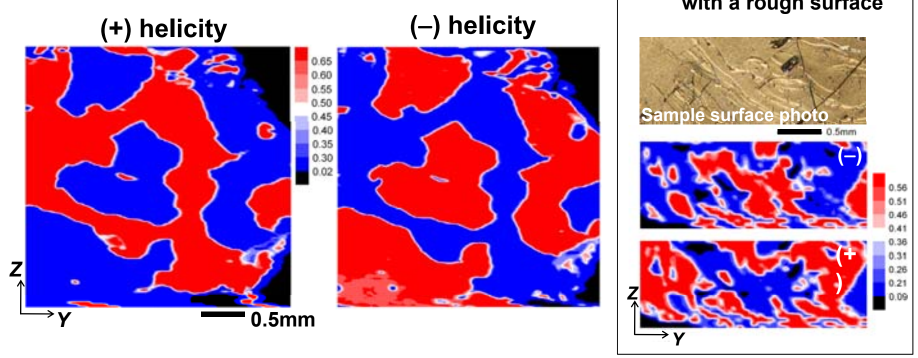

*Red and blue regions correspond to either a left- or right-handed spin-chiral monodomain.

*The observed domains are irregular in shape with a size on a submilimeter scale.

*There is a tendency that the domain boundaries are clamped at surface defects.

*The observed domains were apparently smaller in size than those on a smooth surface.

Thermal effect on the spin-chiral domain structure in $Ba_{0.5}Sr_{1.5}Zn_2Fe_{12}O_{22}$

Hiraoka et al., PRB (in press)

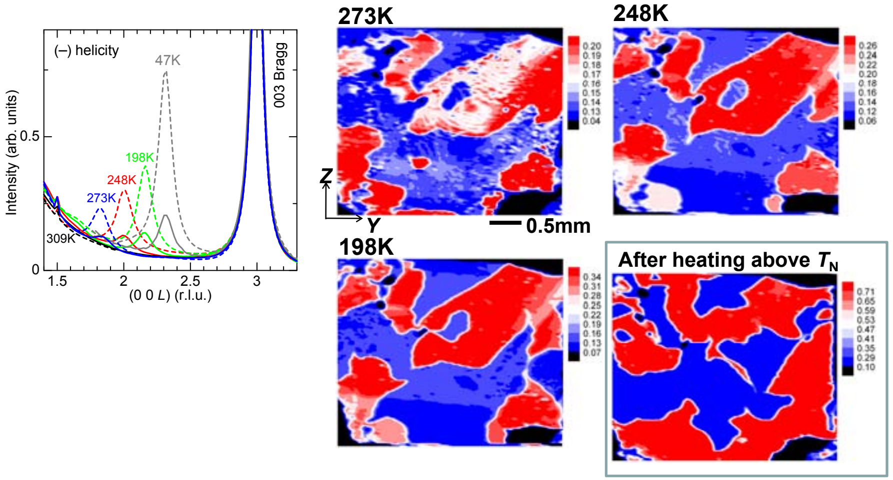

The domain structure is robust with respect to the variation of T and time once they are formed, but is not reproducible once the crystal is heated above T_N.

Outline of this lecture

- Symmetry in crystals
- Magnetic symmetry
- Conventional magnetoelectric effect
- Single crystal growth
- Spin-spiral-driven multiferroics
  - Orthorhombic perovskite manganites $RMnO_3$
  - Cuprates and ferrites working at room temperature
- Observation of spin-spiral domain structure
- ME effect in magnetically-disordered system

with Y. Yamaguchi (Osaka), T. Nakano(Osaka), Y. Nozue (Osaka)

To purse the ME coupling owing to multi-spin variables such as spin chirality and toroidal moment in magnetically-disordered systems

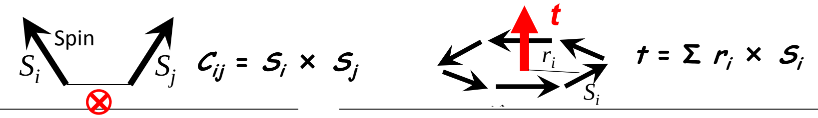

Magnetically-induced ferroelectricity & Vector spin chirality

- **Ferroelectricity driven by spiral spin order**

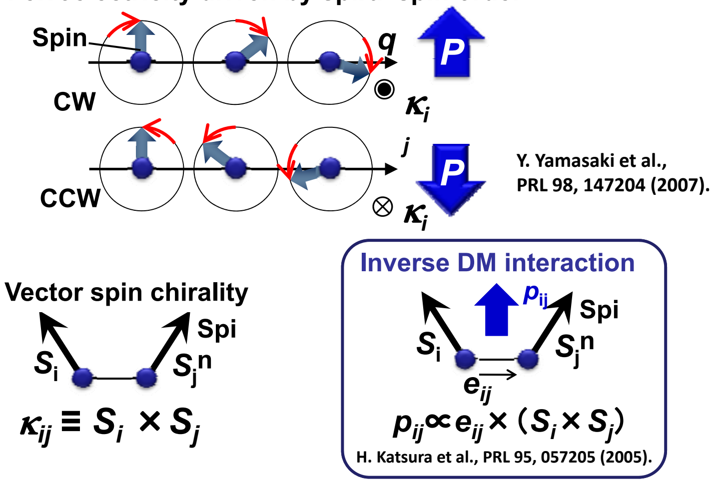

Y. Yamasaki et al., PRL 98, 147204 (2007).

✓ Polarization P ⇔ Chirality κ_{ij}

Vector spin chirality can be detected as electric polarization P through ME coupling.

By recent development of multiferroics research,

Strong correlation between spin frustration & magnetoelectric coupling has been well recognized.

Magnetoelectric effect is useful to detect

Vector spin chirality $\kappa = S_i \times S_j$

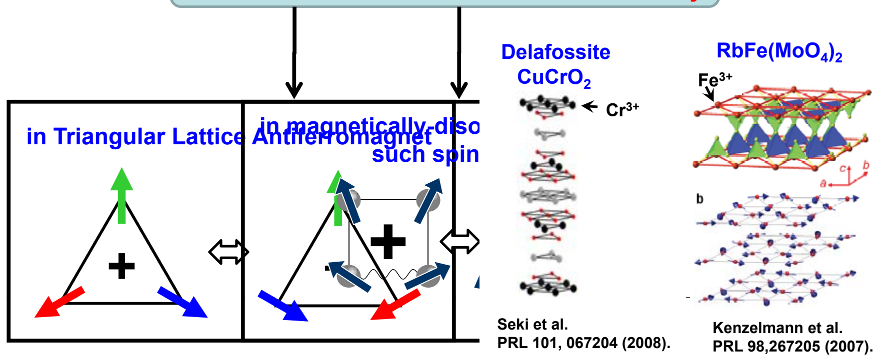

Theoretically, multi-spin variables can be nonzero even in the absence of long-range magnetic order.

Chiral spin liquid phase in helimagnets

F. Cinti et al., PRL 100, 057203 (2008); PRB 83, 174414 (2011).

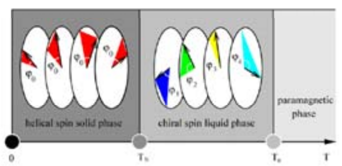

FIG. 1 (color online). Schematic representation of Villain's conjecture. In the chiral spin liquid phase, corkscrews all turning clockwise (or all anticlockwise) with in general $\varphi_i \neq \varphi_j$. In the helical spin solid phase, same angle value φ_0 for all spins.

Spin-chirality decoupling in spin-glass system

H. Kawamura, PRL 68, 3785 (2011);
J. Phys. Condens. Matter 23, 164210 (2011).

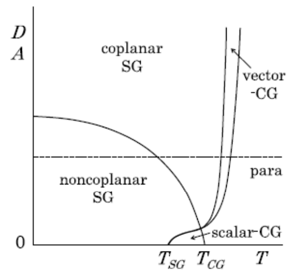

Figure 1. Phase diagram of the *XY*-like SG with an easy-plane-type uniaxial magnetic anisotropy in the uniaxial anisotropy versus the temperature plane. T_{CG} and T_{SG} represent the chiral-glass and the spin-glass transition temperatures of the fully isotropic Heisenberg system.

⇨ **It is possible that ME materials are found in magnetically-disordered phases.**

Spin chirality in spin glass system

A chirality driven mechanism for spin-glass transitions

H. Kawamura, PRL 68, (1992) 3785.

Heisenberg spin glass

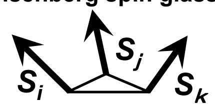

$S_i \cdot (S_j \times S_k)$

Anomalous Hall effect due to scalar spin chirality

T. Taniguchi, et al., PRL 93, (2004) 246605.

XY spin glass

Vector spin chirality can exist.

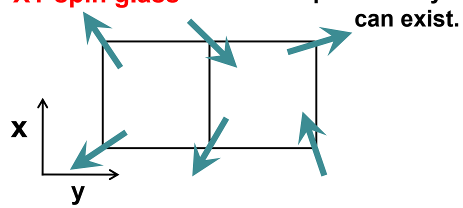

H. Kawamura, J. Phys. Cond. Matter 23, 164210 (2011).

Can we detect vector spin chirality in spin glass system though magnetoelectric coupling?

Example compounds showing insulating & XY-like spin glass state

*$Rb_2Mn_{1-x}Cr_xCl_4$	K. Katsumata et al., PRB 25, 428 (1982).
*$Ni_xMn_{1-x}TiO_3$	A. Ito et al., JMMM 104, 1637 (1992).

Crystal structure of $Ni_xMn_{1-x}TiO_3$

ilmenite structure

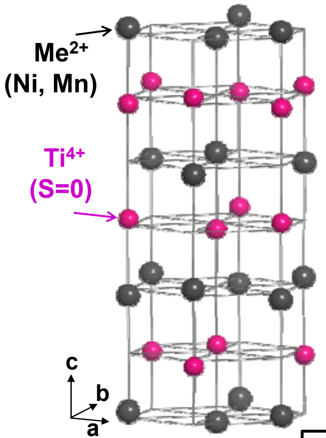

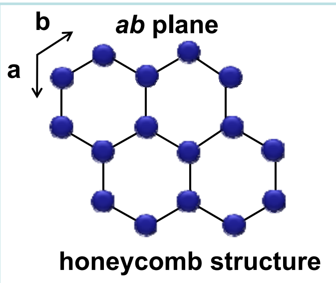

- Alternating stack of Me^{2+} & Ti^{4+}
- Only Me (Ni, Ni) ions are magnetic.
- Space group $R\bar{3}$ ⟶ centrosymmetric

…gram of $Ni_xMn_{1-x}TiO_3$

Ni = 0.42 H. Kawano et al., JPSJ 62, 2575 (1993)

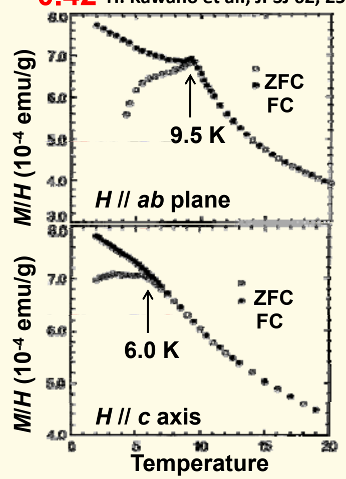

9.5 K : inplane spin component freezes.

6.0 K : *c*-axis spin component freezes.

XY-like Spin Glass

Pseudo vector spin chirality appears at 9.5 K?

…M104-107, 1637 (1992).

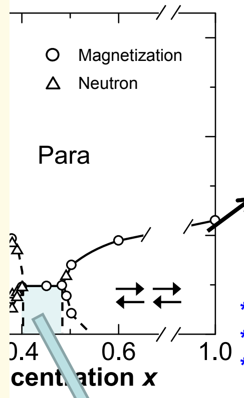

$NiTiO_3$

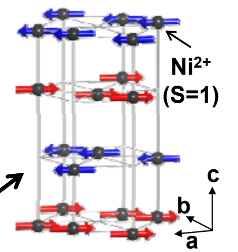

*FM within *ab* plane
*AFM between layers
*easy axis // ab plane

Ni = 0.4~0.5 shows spin glass phase with weak inplane anisotropy.

Our experiments

Sample $Ni_{1-x}Mn_xMnO_3$

Single crystals are grown by the floating zone method.

Phase diagram $Ni_xMn_{1-x}TiO_3$

A. Ito *et al.*, J. MMM 104-107, 1637 (1992).

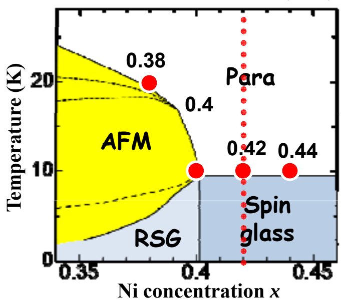

RSG : Reentrant Spin Glass

owing measurements.

② Frequency dependence of ε

Measurements of capacitance with an LCR meter

③ Specific heat in magnetic fields

measured with the relaxation technique (PPMS Option)

④ Composition dependence

- $MnTiO_3$
- $(Ni,Mn)TiO_3$ Ni=0.38, 0.40, 0.42, 0.44

Magnetic & dielectric properties at zero magnetic fields

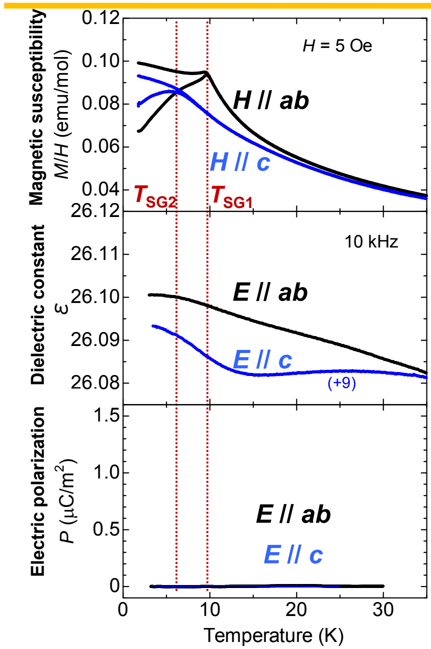

$Ni_{0.42}Mn_{0.58}TiO_3$

Magnetic susceptibility

Anomalies at T_{SG1} ~ 9.5 K

T_{SG2} ~ 6.0 K

Spin glass transition

[consistent with previous study H. Kawano et al., JPSJ 62, 2575 (1993)]

Dielectric properties

No anomaly at T_{SG1} & T_{SG2}

No correlation between magnetic & dielectric properties was observed.

Magnetic field effect on electric polarization in $Ni_{0.42}Mn_{0.58}TiO_3$

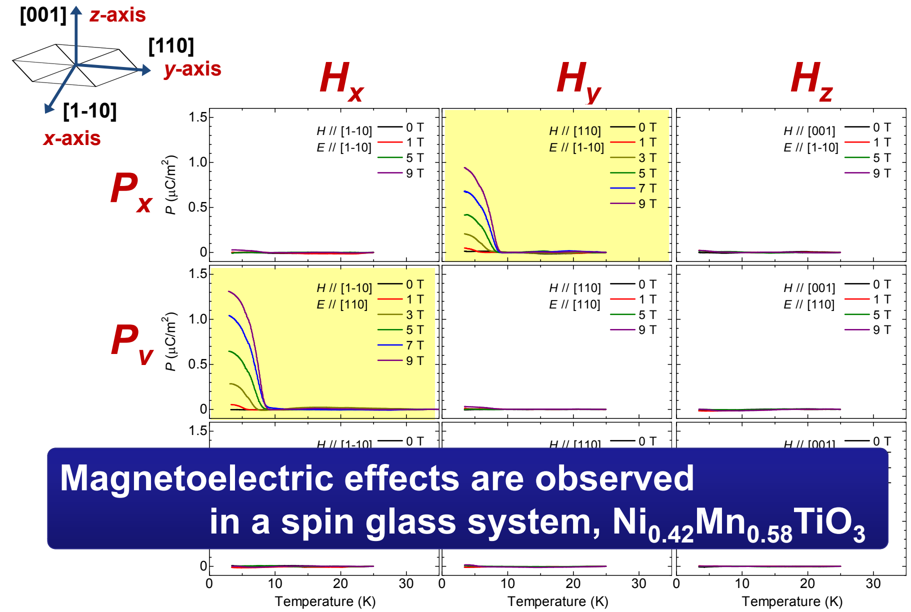

Magnetoelectric effects are observed in a spin glass system, $Ni_{0.42}Mn_{0.58}TiO_3$

Finite polarization appears only in two configurations

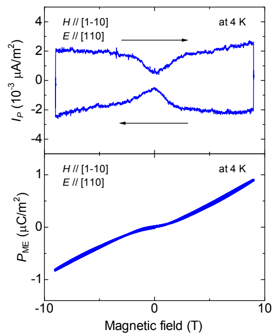

At high *H*, polarization shows almost linear *H* dependence.

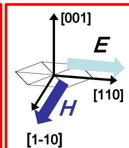

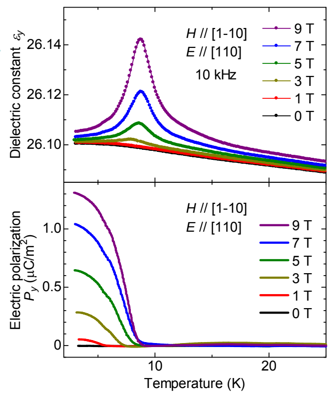

Magnetoelectric coefficient

$$\begin{pmatrix} P_x \\ P_y \\ P_z \end{pmatrix} = \begin{pmatrix} 0 & \alpha_{12} & 0 \\ -\alpha_{12} & 0 & 0 \\ 0 & 0 & 0 \end{pmatrix} \begin{pmatrix} H_x \\ H_y \\ H_z \end{pmatrix}$$

Off-diagonal & Antisymmetric

What is the origin of the ME effect observed in $Ni_{0.42}Mn_{0.58}TiO_3$?

Proposals for possible origins

1. Magnetic-fields induce long range magnetic order which allows ME effect.

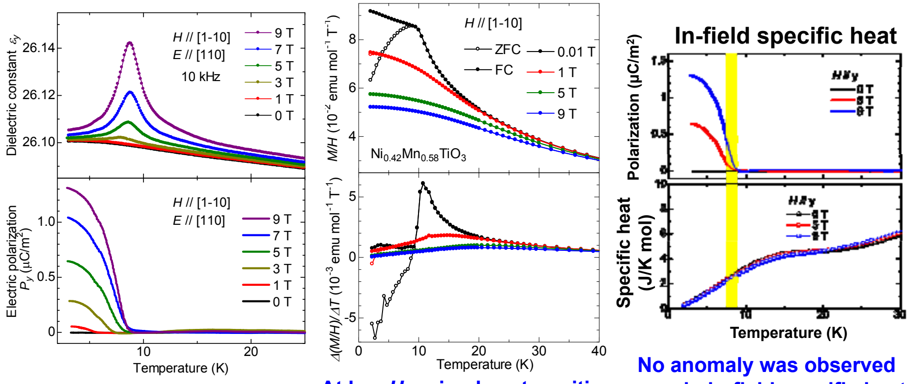

At high *H*, ME effect appears below ~9 K.

At low *H*, spin glass transition appears at 6.0 K & 9.5 K.

No anomaly was observed in in-field specific heat.

No corresponding anomaly was observed in magnetization & specific heat.

Comparison with an Ising-like spin glass system -$Fe_{1-x}Mn_xTiO_3$-

H. Aruga-Katori & A. Ito, JPSJ 62, 4488 (1993)

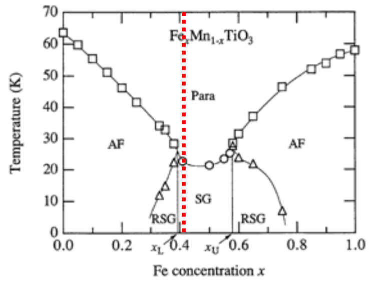

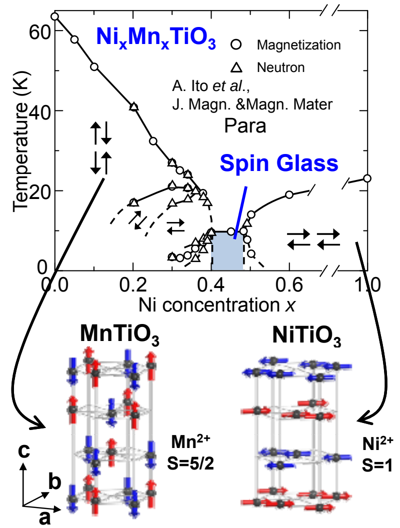

No clear ME anomaly was observ

✓AFM in *c* layer
✓Easy axis // *c*

✓FM in c layer
✓Easy axis ⊥ *c*

Antisymmetric ME effect induced by toroidal moment

2. Toroidal ordering induces ME effect

Toroidal moment *T*

ordered arrangement of magnetic vortic

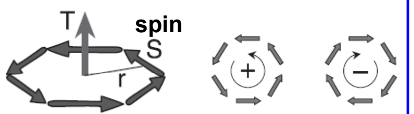

$$T \sim \Sigma_\alpha r_\alpha \times S_\alpha$$

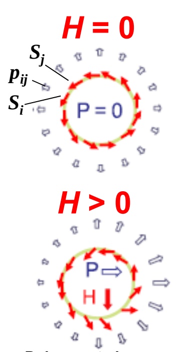

Delaney et al. PRL 102, 157203 (2009).

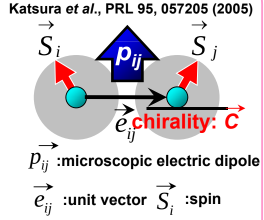

$\vec{p}_{ij}$:microscopic electric dipole

$\vec{e}_{ij}$:unit vector $\vec{S}_i$:spin

$$\vec{p}_{ij} \propto \vec{e}_{ij} \times (\vec{S}_i \times \vec{S}_j)$$

Free energy expression including tor *T* term o

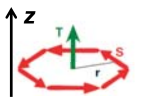

$$F = -P^s{}_iE_i - M^s{}_iH_i - T^s{}_i(\boldsymbol{E}\times\boldsymbol{H})_i \cdots - \alpha_{ij}E_iH_j \cdots$$

consider $T = (0, 0, T_z)$

$$F = -P^s{}_iE_i - M^s{}_iH_i - T_z(E_xH_y - E_yH_x) \cdots - \alpha_{ij}E_iH_j \cdots$$

$$P_x = -\frac{\partial F}{\partial E_x} = P^s{}_x + T_zH_y \cdots + \alpha_{xj}H_j \cdots \qquad P_y = -\frac{\partial F}{\partial E_y} = P^s{}_y - T_zH_x \cdots + \alpha_{yj}H_j \cdots$$

off-diagonal & antisymmetric magnetoelectric effect

A possible toroidal ordering in *XY* spin glass system

① XY spin glass

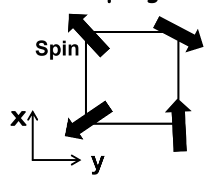

Total *T* = 0

$$T \propto \sum r_i \times S_i$$

E×H induced a finite toroidal moment (spin vortex) through -T(E×H)

"induced" $T_z \neq 0$

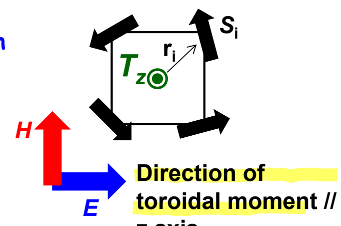

Direction of toroidal moment // z axis

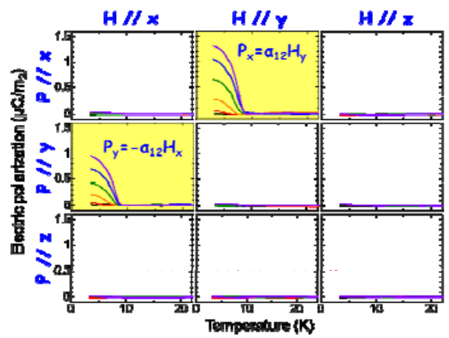

Magnetoelectric cooling procedure (cooling with H & E)

System drop into a valley with $T_z \neq 0$

$$\begin{pmatrix} P_x \\ P_y \\ P_z \end{pmatrix} = \begin{pmatrix} 0 & T_z & 0 \\ -T_z & 0 & 0 \\ 0 & 0 & 0 \end{pmatrix} \begin{pmatrix} H_x \\ H_y \\ H_z \end{pmatrix}$$

Antisymmetric ME effect are induced in XY spin glass

A possible toroidal ordering in ilmenite $Ni_{0.42}Mn_{0.58}TiO_3$

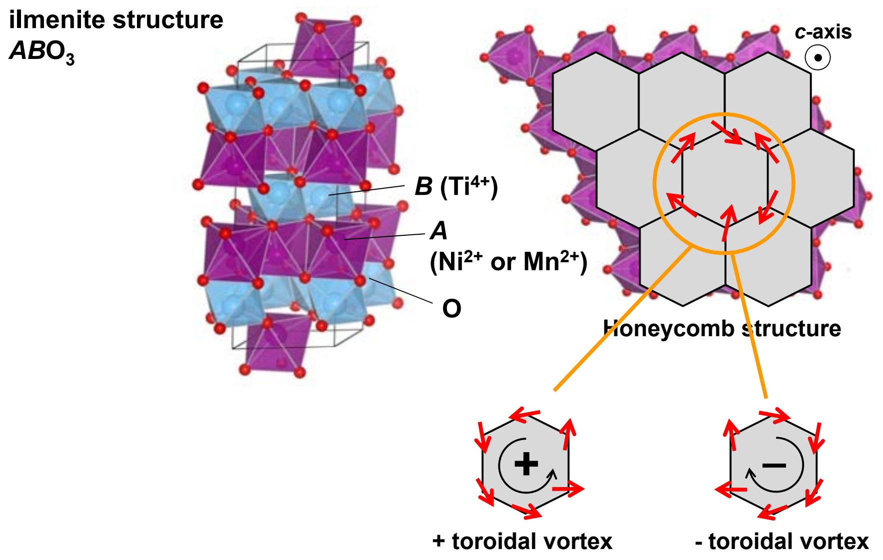

In spin glass, spins randomly freeze.
However, *H* & *E* field cooling
can yield net toroidal moment
and resultant ME effect .

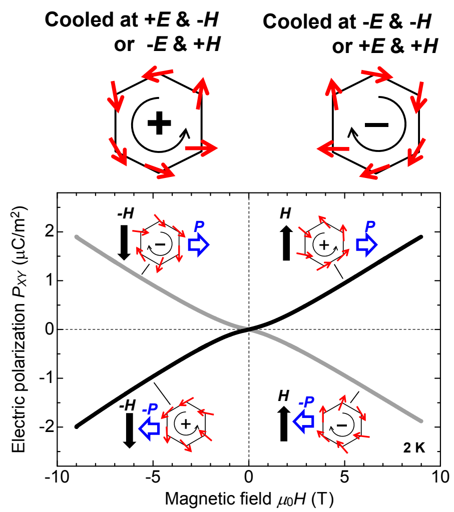

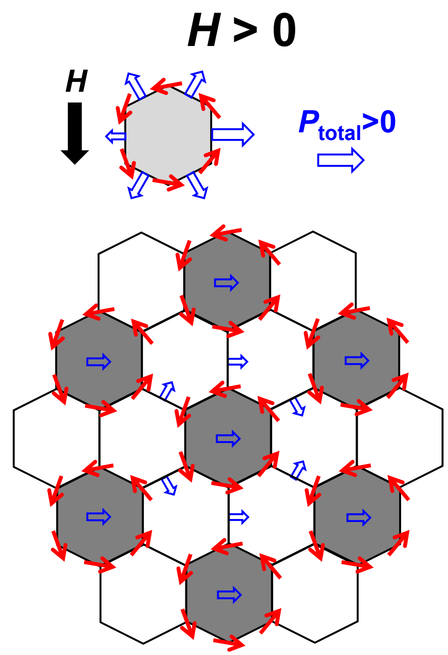

Glassy feature in dielectric constant ε

Frequency dependence of ε

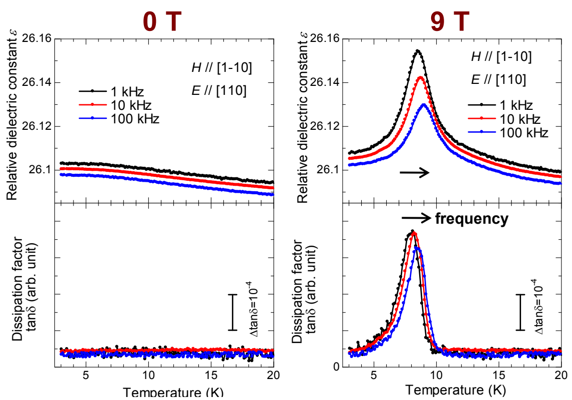

✓ Peaks shifted toward high *T* as the frequency of AC electric fields increased.

c.f. AC χ in spin glass ($Fe_{0.5}Mn_{0.5}TiO_3$)

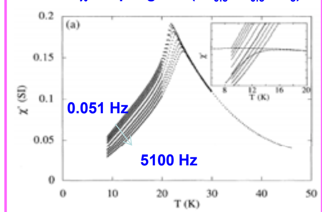

J. Mattsson, et al., PRL 74, 4305, 1995

Relaxor ferroelectrics $Pb(Mg_{1/3}Nb_{2/3})O_3$

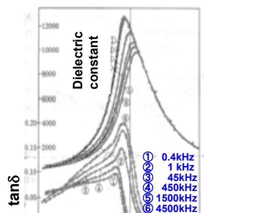

A glassy feature seems to survive in the field-induced state & contribute to the electric polarization.

Effect of ME cooling fields (*E* & *H*) on electric polarization

* measured at *H* = 9T & *E* = 0V/m in x = 0.40 sample

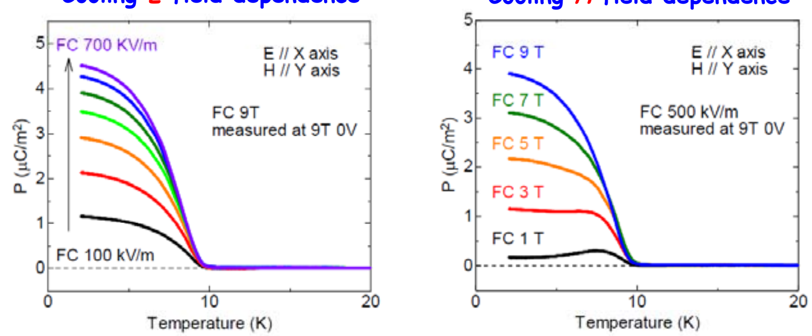

Electric polarization *P* monotonically increases, as cooling *E* & *H* increase.

⇨ *Degree of the alignment of toroidal moments can be tuned by the ME field E × H.*

The behavior may reflect the SG feature in which a resulting state of frozen spins strongly depends on the cooling condition.

Summary (ME effect in a magnetically-disordered system)

ME properties were investigated for an *XY*-like spin glass,
$Ni_xMn_{1-x}TiO_3$ ilmenite structure.

We observed

① **off- diagonal & antisymmetric ME effects,**

② **frequency-dependent dielectric constant,**

③ **no anomaly in specific heat,**
(indicating that long rage ordering wasn't induced by *H*)

$$\begin{pmatrix} P_x \\ P_y \\ P_z \end{pmatrix} = \begin{pmatrix} 0 & T_z & 0 \\ -T_z & 0 & 0 \\ 0 & 0 & 0 \end{pmatrix} \begin{pmatrix} H_x \\ H_y \\ H_z \end{pmatrix}$$

These results were reasonably explained by considering that the spin-freezing process under both *E* & *H* makes toroidal moments polarized.

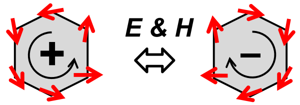

Yamaguchi et al., *PRL* 108, 057203 (2012).

Summary

- Symmetry in crystals
- Magnetic symmetry
- Conventional magnetoelectric effect
- Single crystal growth
- Spin-spiral-driven multiferroics
  - Orthorhombic perovskite manganites $RMnO_3$
  - Cuprates and ferrites working at room temperature

- Observation of spin-spiral domain structure
- ME effect in magnetically-disordered system